Stress-strain-strength-flow parameters from enhanced in-situ tests

Paul W. Mayne
Georgia Institute of Technology, Atlanta, Georgia USA

Proceedings, International Conference on In-Situ Measurement of Soil Properties & Case Histories [In-Situ 2001], Bali,Indonesia, May 21-24, 2001, pp. 27-48.

ABSTRACT: Seismic piezocone penetration tests (SCPTu) with dissipation phases are particularly useful for geotechnical site characterization as they provide four independent readings with depth from a single sounding, as well as time-rate information. The penetration data (q_t, f_s, u_b) reflect failure states of stress, the shear wave (V_s) provides the small-strain stiffness, and dissipations give flow properties. Taken together, an entire stress-strain-strength-flow representation can be derived for all depths in the soil profile. A similar approach is obtainable from seismic flat dilatometer soundings. Methods of evaluating the degree of preconsolidation, stress state, strength, stiffness, and permeability characteristics of sands and clays are reviewed with example applications. For clays, a combined cavity expansion and critical-state model has proven useful. For sands, chamber test results have guided the interpretation of parameters.

1 INTRODUCTION

The complexities of soil behavior are many and include the inherent aspects of natural fabric, anisotropy, nonlinear stress-strain behavior, porewater response, cementation, and sensitivity, as well as rheological effects such as aging, strain rate, creep, and thixotropy. Thus, the overreliance of some in using the single N-value from the standard penetration test to provide most of the geotechnical data needed for engineering analysis is not very realistic. Many varied and useful tests have been developed to measure and assess the in-situ properties and parameters of soils, as discussed in Jamiolkowski, et al. (1985) and Lunne, et al. (1994). Of particular note is the seismic piezocone penetrometer test (SCPTu) that is a hybrid field method, combining the virtues of the CPT with downhole geophysics (Robertson, et al., 1986), as illustrated in Figure 1. In a similar manner, the seismic flat dilatometer (SDMT) provides both penetration and wave velocity data from the same sounding (Hepton, 1988).

The SCPTu and SDMT obtain measurements at two opposite ends of the stress-strain spectrum, including failure states corresponding to the strength characteristics (τ_{max}) of the material, as well as the nondestructive properties associated with elastic wave propagation and soil stiffness (E or G). In addition, both of these tests can also be halted periodically to monitor the decay rate of readings with time. This is particularly advantageous in fine-grained soils, where excess porewater pressures are induced by the installation of the probe. These readings provide direct information about the flow properties of the soil, namely the coefficient of consolidation and permeability.

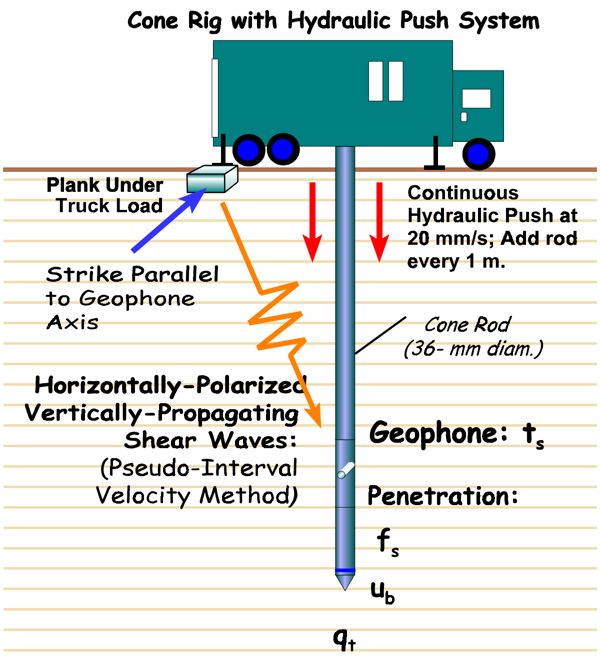

Figure 1. Setup and procedure for seismic piezocone testing

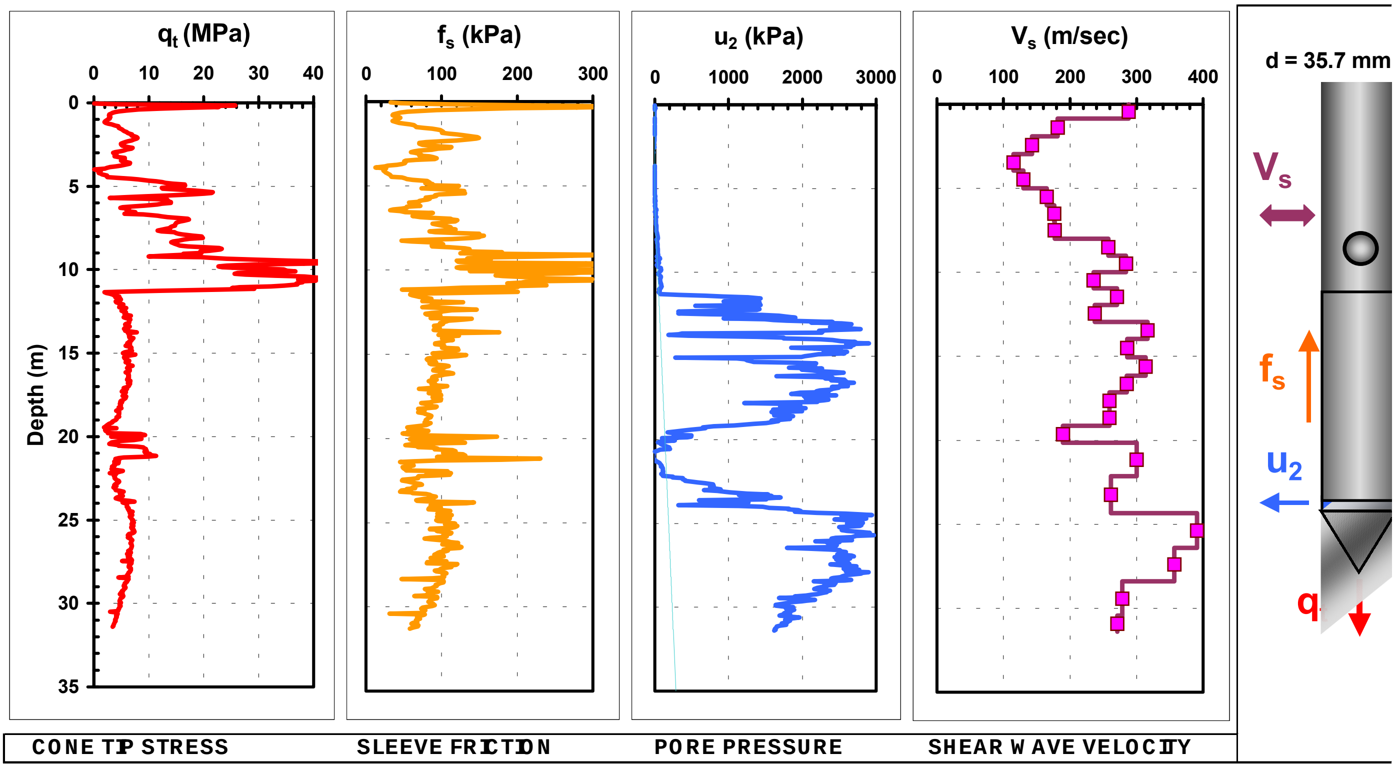

Figure 2. Illustrative results of SCPTu for geostratigraphic profiling of soil layers in Memphis, Tennessee.

Of interest to geotechnical exploration, the SCPTu and SDMT provide optimization of data collection for geostratigraphy and the evaluation of soil parameters.

1.1 *Geostratigraphic profiling*

The cone penetrometer provides continuous readings with depth, thus is unsurpassed in its ability to delineate changes in soil strata, layer boundaries, and the presence of seams, lenses, and inclusions. The basic readings include: cone tip stress (q_c), sleeve friction (f_s), and penetration porewater pressures (u). An example of the detailed profiling capability is shown in Figure 2 for Memphis, Tennessee, which indicates an 11-meter thick sand layer overlaying a double marine clay layer. The unusual feature at 20 to 22 m depth is believed to be a buried desiccated crust of the lower clay unit.

A visual examination of the individual penetration records is often sufficient for determining stratigraphy and soil classification. If necessary, the use of empirical soil behavioral charts can be implemented, such as that by Robertson (1990).

1.2 *CPT measurement corrections*

The tip stresses must be corrected for porewater effects on the back of the cone tip (Lunne et al., 1997), thus designated q_T. This correction requires the porewater pressures to be measured at the shoulder (u_b or u_2), therefore, this is the standard piezocone geometry. The tip stress correction is paramount for soundings taken in soft to firm to stiff intact clays where positive Δu are generated. In the case of sands where pore pressures are near hydrostatic ($u_2 \approx u_0$) and much smaller than q_c, the correction is often small (therefore, $q_T \approx q_c$). In the special case of fissured and overconsolidated materials, the measured u_b can be zero or negative, again diminishing the need for correction. In this situation, a midface porewater pressure element (u_t or u_1) provides more interesting data for stratigraphic mapping (Mayne, et al. 1995).

A similar correction occurs for sleeve readings, yet is not demanded from a practical standpoint because additional channels of porewater pressures must be obtained (Jamiolkowski, et al., 1985).

A nice feature concerning porewater readings is that corrections are not required, provided that proper saturation techniques are followed and clogging of the filter does not occur. In general, plastic porous filters saturated under vacuum with glycerine are excellent for the shoulder element. Other filter types include ceramic, sintered brass, and steel, that can be saturated with water, silicon, and/or special greases (Campanella & Robertson, 1988).

The importance of taking accurate baseline readings before and after each sounding should be noted. As electronics in both the penetrometer and field data acquisition unit can be affected by changes in temperature, humidity, electromagnetic interference, power drops/surges, and other happenstance, initial baseline values of each channel must be carefully established prior to advancing the sounding.

Finally, the use of different class penetrometers should be considered with regard to data interpretation, especially on critical projects or where high-quality results are expected. The use of class 1 cones are sufficient for routine exploration of subsurface strata and layering sequences across a site, yet the interpretation of soil parameters and properties may necessitate a class 3 penetrometer (Lunne, et al. 1997) at select sounding locations for calibration and verification with laboratory triaxial shear, consolidation, and resonant column results.

1.3 *DMT measurement corrections*

The flat plate dilatometer provides two pressure readings at either 20-cm or 30-cm depth intervals: contact pressure (“A”) and expansion pressure (“B”). Both readings require a correction for the membrane stiffness taken in air, per Schmertmann (1986). The corrected “A” and “B” are designated p_0 and p_1, respectively.

1.4 *Corrections to geophysical data*

With modern electronics, the early-reported problems of timing delays associated with trigger switches and oscilloscopes now appear minimized. For pseudo-interval downhole tests conducted with a single horizontal geophone, the individual wave trains from the geophysical surveys do require an assessment of the shear wave arrivals that are made difficult, however, due to the pre-arrival of the P-wave (Campanella, 1994).

Traditionally, the identification of the S-wave arrival has relied upon polarized wave-generation and paired sets of right & left strikes to assess a single point on the time of arrival (t_s). Today, with available software packages such as Mathcad, it is relatively simple to conduct cross-correlation over thousands of points on the wave train to evaluate the interval time. This then represents a correction in data evaluation procedures. Of course, the true-interval method with two downhole geophones approach (e.g., Burghignoli, et al. 1991) avoids this issue and with the advent of new digital cones, may in fact become the future manner for SCPTu.

Since the same energy source is used for each separate event, as downhole tests advance with depth, the amplitude of the wave arrival decreases, thus the shear strain can be measured as the peak particle velocity divided by the shear wave velocity, $\gamma_s = \mathring{u}/V_s$. As such, a correction for the derived small-strain shear modulus ($G_0 = \rho_T V_s^2$) based on the measured strain level is available (Larsson & Mulabdić, 1991a).

2 SOIL STRENGTH

For saturated geomaterials, it is common to assume that either the *drained strength* or *undrained strength* conditions prevail during penetration. For clean sands, fully-drained penetration is the usual consideration with direct assessment focused on the effective stress friction angle (ϕ') and an assumed nil value for the effective cohesion intercept ($c' = 0$). For clays, total stress analyses with no volume change are the normal assumptions, with penetration data giving the undrained shear strength (c_u or s_u).

The undrained strength of soil is greatly affected by many factors, including initial stress state (K_o), anisotropy, boundary conditions, strain rate, direction of loading, degree of disturbance, and other variables. Because of its non-uniqueness for a given clay, it is best to relate in-situ test results to a more stable parameter. Consequently, it is recommended that the preconsolidation stress (σ_p') obtained from laboratory one-dimensional consolidation (oedometer) tests be used as a unique and consistent reference for benchmarking in-situ penetration test data in clays. Then, the normalized form, or overconsolidation ratio ($OCR = \sigma_p'/\sigma_{vo}'$), can be related to a suite of undrained strengths via either an empirical stress history approach (Ladd, 1991) or constitutive relationships, such as critical state soil mechanics (Wroth, 1984).

2.1 *Drained strength of sands*

The drained strength of sands can be expressed in terms of the Mohr-Coulomb criterion as a peak friction angle (ϕ'). Here, perhaps, the standard penetration test (SPT) can be used, provided that energy corrections are made properly to the measured N-values. Energy measurements from donut, safety, and auto-hammers show, on average, an energy efficiency of 60%, yet this varies with operator, equipment, and practice in a particular country.

Recent findings from high-quality frozen sand specimens and associated N-values in soil borings have been reported by Hatanaka & Uchida (1996). These results have been adjusted from the Japanese 78% efficiency to an equivalent 60% value (designated N_{60}) and normalized to a stress-level of one atmosphere, designated $(N_1)_{60}$, and related to the triaxial-measured value of ϕ', as shown by Figure 3.

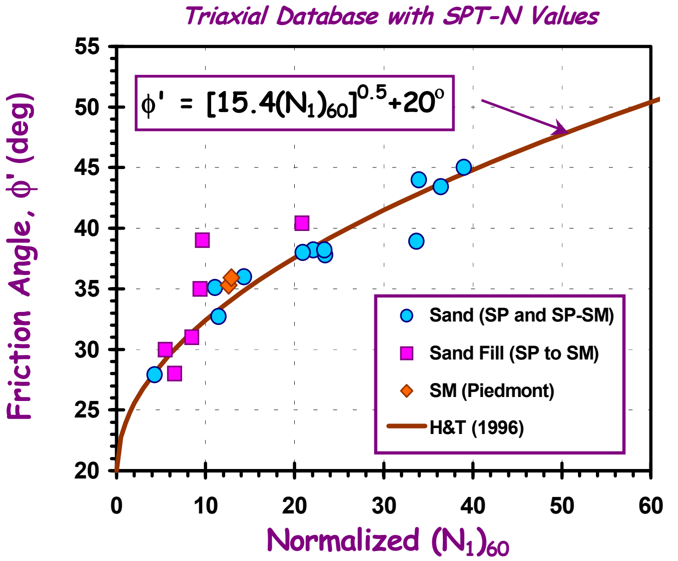

Figure 3. Peak friction angle of sands from SPT data. (Modified after Hatanaka & Uchida, 1996).

Additional results from residual silty sand in Atlanta, Georgia (30% fines) reported by Mayne (1998) have also been included and appear to fit this relationship. The expression for peak ϕ' is given by:

$$\phi' = 20° + \sqrt{15.4(N_1)_{60}} \qquad (1)$$

where the energy-corrected and stress-normalized N-value is obtained from:

$$(N_1)_{60} = \frac{N_{60}}{(\sigma_{vo}'/\sigma_{atm})^{0.5}} \qquad (2)$$

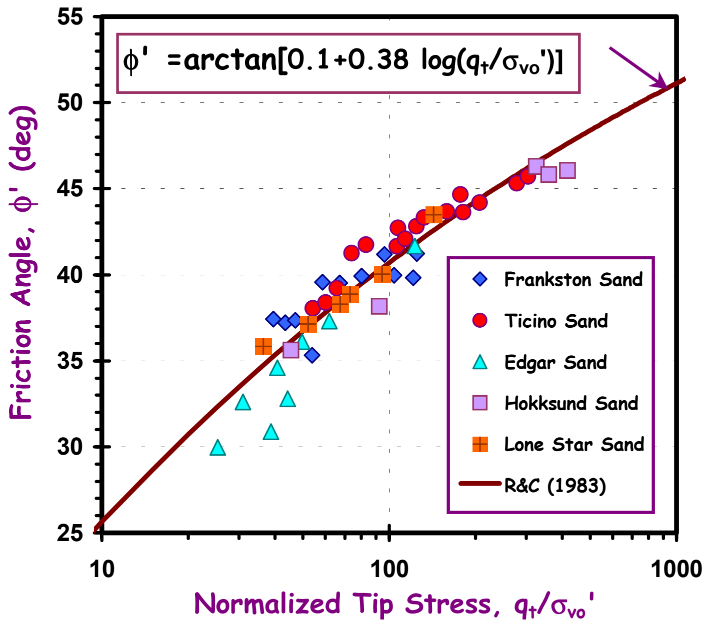

Figure 4. Peak friction angle of clean quartz sands from CPT (after Robertson & Campanella, 1983).

The parameter σ_{atm} = 1 bar = 100 kPa = reference stress equal to one atmosphere.

For the CPT, several separate theories of bearing capacity and wedge plasticity were evaluated in light of calibration chamber test data from several quartz sands that were compiled by Robertson & Campanella (1983). The recommended relationship for unaged, uncemented quartz sands is shown in Figure 4. The expression for peak ϕ' from CPT is given by:

$$\phi' = \arctan [0.1 + 0.38 \log (q_c/\sigma_{vo}')] \qquad (3)$$

that shows good agreement between experimental results and the equation. In essence, this is an inverse solution to the well-known bearing capacity factor for a deep foundation: $N_q = q_c/\sigma_{vo}' = fctn(\phi')$. Yet, for clean sands, it has been observed experimentally that the measured tip resistance increases in proportion to the square root of effective overburden stress (e.g., Olsen, 1994).

An alternative expression that accounts for the nonlinear normalization of q_c with stress level and consistent with (1) has been proposed (Kulhawy & Mayne, 1990):

$$\phi' = 17.6° + 11.0 \log(q_{c1}) \qquad (4)$$

where $q_{c1} = (q_c)/(\sigma_{vo}'/\sigma_{atm})^{0.5}$ = normalized cone tip resistance. For the silty sand [Piedmont geology], (4) provides excellent agreement with consolidated triaxial tests on recovered samples (Figure 5). Two commercial labs gave consistent results with characteristic parameters: $c' = 0$ and $\phi' = 35°\pm1°$.

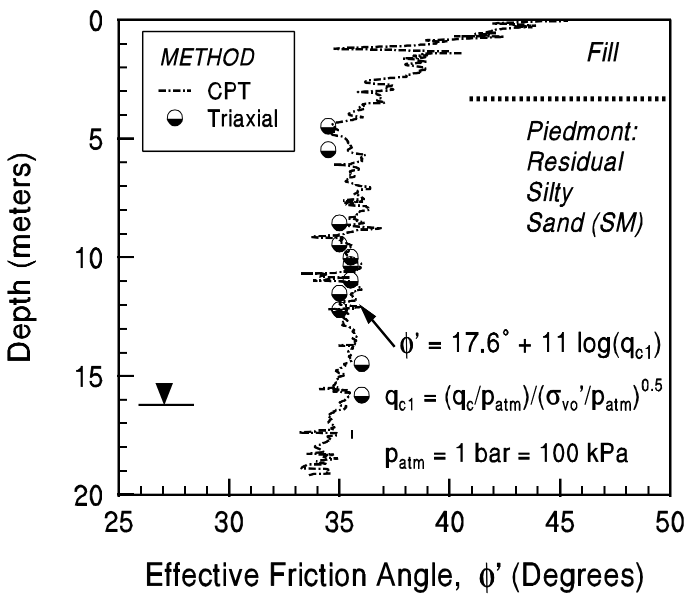

Figure 5. CPT profiling of ϕ' in silty sand (30% fines) in Atlanta, Georgia, USA.

The peak angle of friction in sands can also be assessed by flat plate dilatometer tests. A wedge plasticity solution for the CPT was presented by Marchetti (1985) that was later cross-correlated for CPT-DMT relationships by Campanella & Robertson (1991). The wedge solutions relate the DMT lateral stress index (K_D) as a function of ϕ' and lateral stress state, including active, at-rest (NC), and passive conditions. For this approach, the passive case appears to provide a generally conservative evaluation of peak ϕ' when compared with a data from three field sites (see Figure 6). Results from the silty sand appear low in this case and perhaps affected by capillarity effects in the soil.

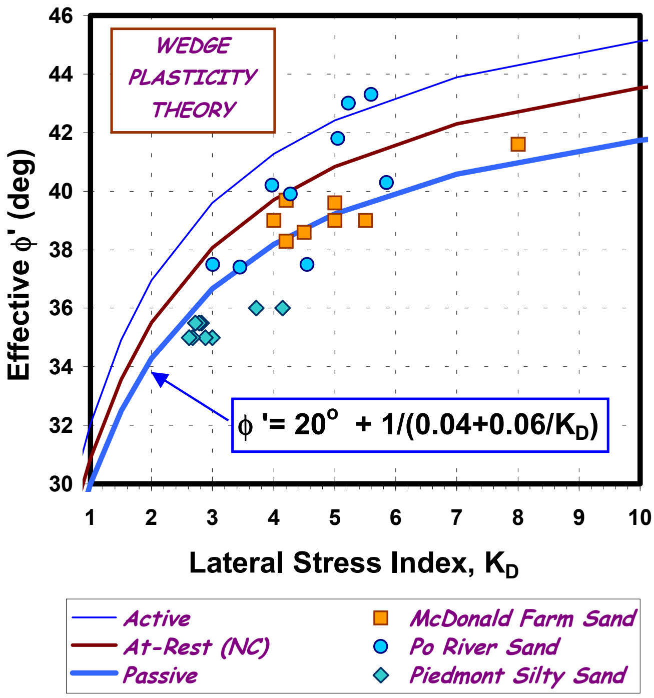

Figure 6. Evaluation of peak ϕ' of sands from DMT data (Modified after Marchetti, 1997).

The expression for the K_p case can be approximated by a hyperbola of the form:

$$\phi' = 20° + \frac{1}{0.04 + 0.06/K_D} \qquad (5)$$

where $K_D = (p_0\text{-}u_0)/\sigma_{vo}'$ = lateral stress index.

2.2 *Effective Strength of Soils*

Of special interest is the possibility in evaluating the effective stress strength parameters of all soil types from the CPT, since porewater pressures are measured. An effective stress formulation coupled with plasticity

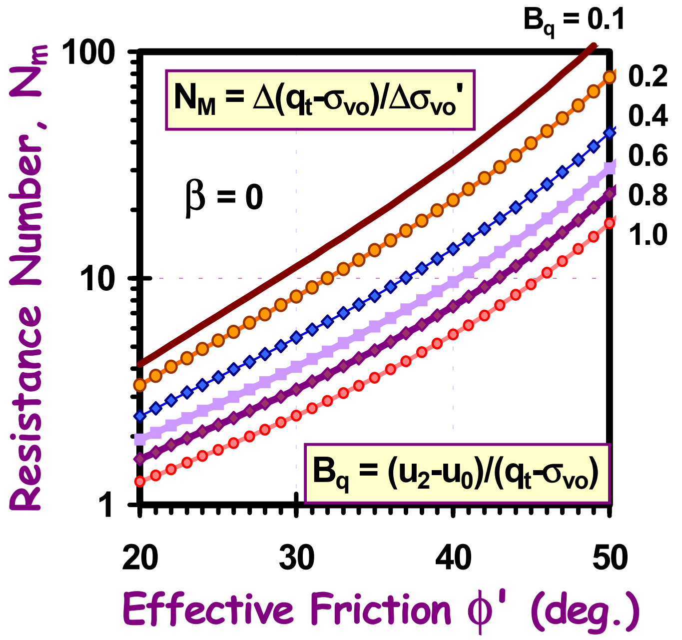

Figure 7. Effective stress parameter determination for all soil types from CPTu data (Senneset, et al. 1989).

theory for interpretation of piezocone data has been developed that relates effective ϕ' to the cone resistance number ($N_m = \Delta q_{net}/\Delta\sigma_{vo}'$) and normalized porewater pressure parameter ($B_q = \Delta u_2/\Delta q_{net}$), where $q_{net} = (q_t\text{-}\sigma_{vo})$. Figure 7 shows a summary graph for one case and full details on the calculations are given elsewhere (e.g., Senneset, et al., 1989).

2.3. *Undrained strength of clays & silts*

The undrained shear strength (s_u, also c_u) is a total stress parameter that is often used in defining the relative consistency of fine-grained soils. The old archaic term "cohesion" (c) should no longer be used, as it results in confusion with the effective cohesion intercept (c′).

The undrained shear strength depends on initial stress state, direction of loading, rate, stress history, degree of fissuring, boundary conditions, and other factors. Each laboratory test (i.e., triaxial, plane strain, simple shear) provides a different value of s_u on the same clay because of these effects. Moreover, each of the in-situ tests is traditionally assessed using a different theoretical basis in order to interpret s_u. For instance, limit equilibrium is applied to vane shear tests to obtain s_u from maximum torque readings, whereas cavity expansion theory is used to get s_u from pressuremeter tests. The result is that a matrix of interrelationships and calibrations would be required to connect all of the various laboratory strength modes to the individual in-situ tests. Instead, a stress history approach is followed herein.

The normalized undrained shear strength to effective overburden ratio (s_u/σ_{vo}') has been related to overconsolidation ratio (OCR) both experimentally (e.g., Ladd, 1991) and theoretically (e.g., Wroth, 1984). Extensive calibration efforts have been made using data from triaxial compression (CIUC and CAUC), triaxial extension (CIUC and CAUE), plane strain active (PSA) and extension (PSE), and direct simple shear (DSS), as well as special cuboidal triaxial and hollow cylinder tests (Kulhawy & Mayne, 1990). In as much as the modified Cam Clay has an isotropic yield surface, the distinction between compression and extension type loadings cannot be made without more rigorous considerations, a hybrid Wroth-Prevost model was produced to represent the interrelationships between the laboratory shearing modes, as indicated by Figure 8.

The isotropically-consolidated undrained triaxial compression test (CIUC) with porewater pressure measurements should be considered the minimum level of effort to be undertaken in the lab characterization of s_u. The CIUC provides a direct measurement of both a total stress parameter (s_u) as well as effective stress parameter (ϕ'). Anisotropically -consolidated triaxial, plane strain, simple shear, and extension modes generally require a relatively high level of technical expertise. Since most commercial labs can conduct CIUC tests, this provides a convenient and practical reference. The s_u from CIUC tests are the highest, however, and should be reduced appropriately via Figure 8.

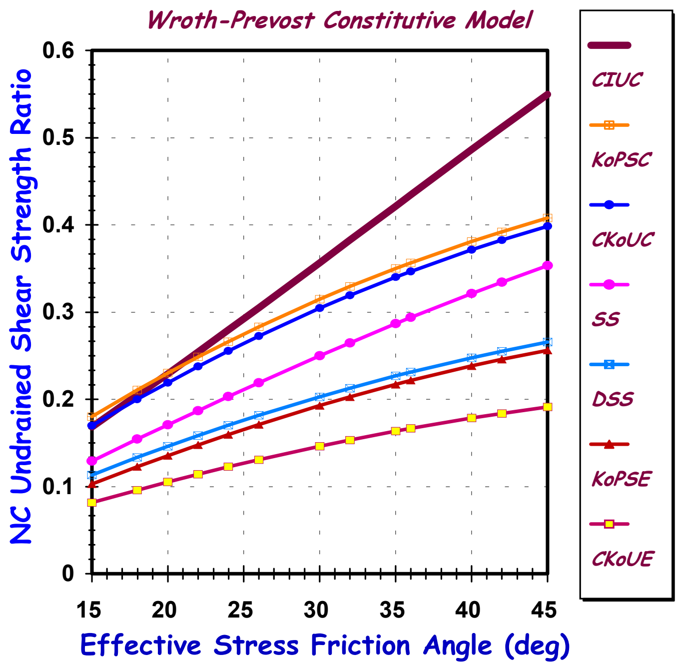

Figure 8. Normalized $(s_u/\sigma_{vo}')_{NC}$ ratios with effective ϕ' from Wroth-Prevost calibrated model.

An internally-consistent critical-state model by Ohta, et al. (1985) provides similar interrelationships for different testing methods. Assuming the normally-consolidated at-rest state can be approximated by K_0 (NC) = 1 - sinϕ', the anisotropic bullet Cam-clay model gives the curves shown in Figure 9.

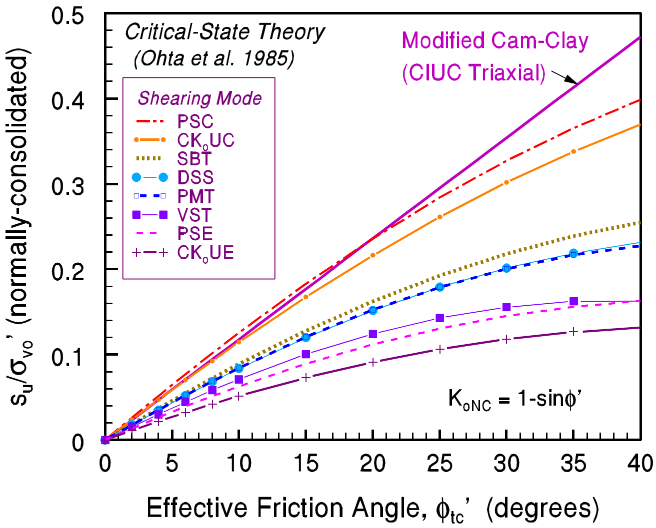

Figure 9. Normalized $(s_u/\sigma_{vo}')_{NC}$ ratios with effective ϕ' from Ohta critical-state model compared with modified Cam-clay.

Thus, a hierarchy of undrained strength ratios can be considered for a given clay, depending on the proper loading case. For each mode, the overconsolidated strength is obtained from:

$$(s_u/\sigma_{vo}')_{OC} = (s_u/\sigma_{vo}')_{NC}\ OCR^{\Lambda} \qquad (6)$$

where $\Lambda = 1 - \kappa/\lambda$ = plastic volumetric strain ratio, $\lambda = C_c/2.3$ = isotropic compression index, $\kappa \approx C_s/2.3$ = isotropic swelling index. For many clays of low to medium sensitivity, a value of $\Lambda \approx 0.8$ is appropriate, while for highly structured and/or cemented clays, a value of $\Lambda \approx 0.9+$ may apply, yet for remolded and/or artificial materials, lower values are found (e.g., for Weald clay, $\Lambda \approx 0.6$).

If the CIUC test is adopted as a reference value, then the undrained strength of intact clays can be represented in terms of stress history and effective stress by (Wroth & Houlsby, 1985):

$$(s_u/\sigma_{vo}')_{CIUC} = (M/2)\ (OCR/2)^{\Lambda} \qquad (7)$$

where $M = 6\sin\phi'/(3-\sin\phi')$ in triaxial compression. For fissured geomaterials, consideration should be given to reducing the strength given by (7) by up to a factor of 2, depending on the extent of cracking and discontinuities. An additional adjustment for strain rate can also be made (Kulhawy & Mayne, 1990).

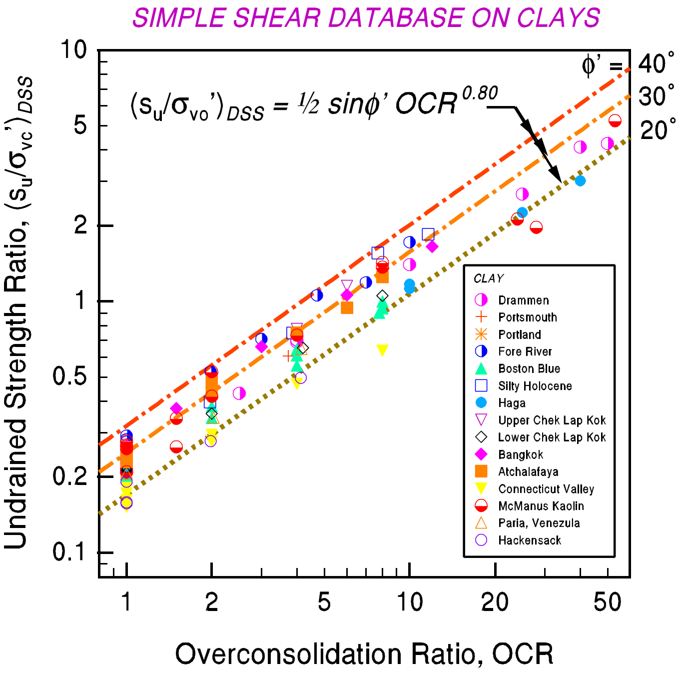

Figure 10. Undrained DSS strength ratio with OCR and ϕ′

For many cases, the appropriate mode of undrained strength (TX, PS, DSS) will not be known beforehand, particularly during the time of the site characterization phase. In these cases, the simple shear is considered a representative and intermediate value that can be used in engineering analyses involving embankment stability, foundation bearing capacity, and excavation problems. A simplifed expression for the DSS mode is given by:

$$(s_u/\sigma_{vo}')_{DSS} = \tfrac{1}{2}\sin\phi'\ OCR^{\Lambda} \qquad (8)$$

The calibration of (8) with data from a variety of clays is shown in Figure 10 and seen to be reasonable.

3 STRESS HISTORY

As the stress history is needed for obtaining s_u in clays and silts, the utilization of in-situ test data will now focus towards the interpretation of the OCR of the formation. Statistical trends and correlative methods have been reported elsewhere based on regression analyses of databases collected by piezocone (e.g., Larsson & Mulabdić, 1991b; Chen & Mayne, 1996), flat dilatometer (Pool, 1994), field vane (Mayne & Mitchell, 1988), as well as other devices (Mayne, 1995). Herein, an analytical model based on cavity expansion and critical-state concepts will be reviewed to express the OCR in terms of piezocone and flat dilatometer results.

3.1 *Piezocone evaluation of OCR in clays*

The cone tip stress can be formulated in terms of the Vesić spherical cavity expansion theory:

$$q_T = \sigma_{vo} + s_u\,[(4/3)(\ln I_R + 1) + \pi/2 + 1] \qquad (9)$$

where $I_R = G/s_u$ = rigidity index, and G = shear modulus at the appropriate level of strain. For the solution, the undrained strength from critical-state soil mechanics given by (7) has been used.

The measured excess porewater pressures are represented as a combination of changes due to octahedral (normal) stresses and shear-induced response:

$$\Delta u_{meas} = \Delta u_{oct} + \Delta u_{shear} \qquad (10)$$

The normal stress component is associated with a large failure zone of soil that is disturbed around the probe and represented by spherical cavity expansion:

$$\Delta u_{oct} = (4/3)\, s_u\ \ln I_R \qquad (11)$$

For spherical cavities, the size of the zone of plastic disturbance is given by $r_{plastic}/r_{probe} = (I_R)^{0.33}$.

The shear component is an interface value that reflects a thin annulus zone that is highly-sheared immediately adjacent to the probe as it punches through the clay. For a piezocone with midface filter element (type 1), the shear term was originally neglected but later was modified (Mayne & Chen, 1994). For shoulder filter elements (type 2), the shear component is evaluated from CSSM:

$$\textit{Type 1:}\quad \Delta u_{shear} \approx 2\,\sigma_{vo}' \qquad (12)$$

$$\textit{Type 2:}\quad \Delta u_{shear} = \sigma_{vo}'[1 - (OCR/2)^{\Lambda}] \qquad (13)$$

The above can be collected and rearranged to express the overconsolidation ratio in terms of a normalized form of the effective cone tip resistance, $(q_T - u)/\sigma_{vo}'$, and material constants M and Λ (Mayne, 1991, 1993):

$$Type\ \ 1:\ OCR = 2\left[\frac{1}{1.95 \cdot M}\left(\frac{q_T - u_1}{\sigma_{vo}'} + 1\right)\right]^{1/\Lambda} \qquad (14)$$

$$Type\ \ 2:\ OCR = 2\left[\frac{1}{1.95 \cdot M + 1}\left(\frac{q_T - u_2}{\sigma_{vo}'}\right)\right]^{1/\Lambda} \qquad (15)$$

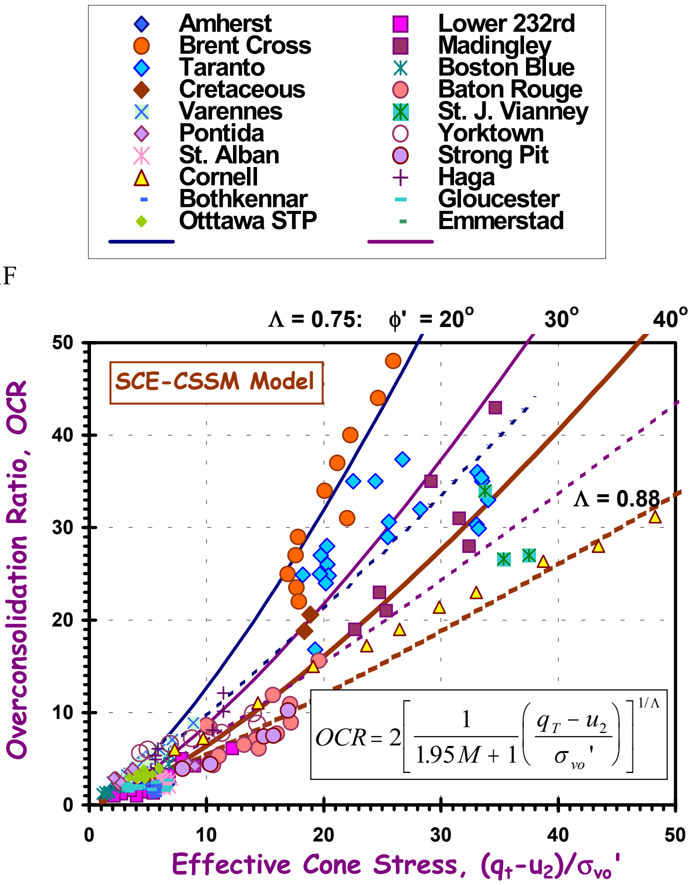

erugiF

11. Analytical model for evaluating OCR from type 2 piezocone data in clays.

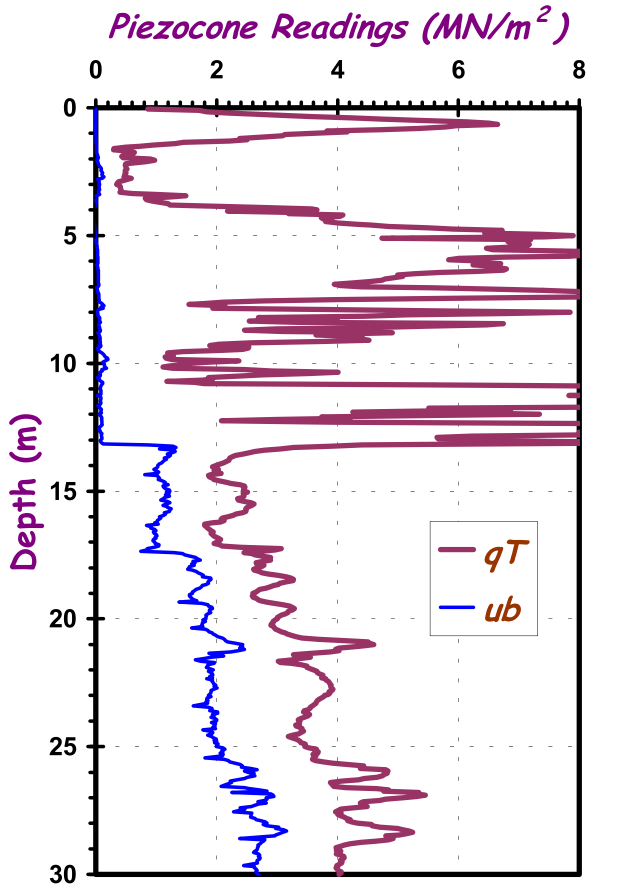

Fig
ure
12. Piezocone data for Cooper River Bridge in South Carolina indicating marl below depths of 13 meters.

The use of (15) for the direct assessment of degree of overconsolidation ratio in clays from type 2 CPTus is shown in Figure 11 for 20 clay sites. Parametric ranges of the input parameters are shown for $20° < \phi'$ $< 40°$ and $0.75 < \Lambda < 0.88$.

It should be emphasized that a class level 3 penetrometer will be most valued as a quality instrument in providing OCRs in clay deposits because of the high accuracy of numbers needed. In this situation, a type 1 cone cannot provide the accurate correction of tip stresses, particularly in soft clays. Moreover, because of the general closeness of the q_T and u_1 readings, the use of (14) may result in some instability of estimates, excepting very stiff to hard overconsolidated and/or fissured materials where the correction for q_T may actually be small and/or the difference between q_T and u_1 is large. When in doubt, always conduct type 2 soundings first to determine the level of the correction.

Results from the ongoing Cooper River Bridge project in Charleston, South Carolina will be presented using a class 3 cone. Figure 12 shows the measured profiles of q_T and u_2 with depth. Of particular interest is the clay deposit encountered below depths of 13 m. This marine deposit is locally termed "Cooper Marl" and consists of a sandy calcareous plastic clay of Oligocene age. Groundwater is about 1 m deep. The marl has an average 40 percent sand fraction that is composed of highly- broken shell fragments. Over the depth range encountered from 13 m to the final investigation depths of 60 m, a summary of the index properties are given in Table 1. The percent of $CaCO_3$ ranges between 50 to 80 percent.

A fairly comprehensive set of consolidated triaxial tests (CD and CU) indicated a consistently high effective stress friction angle of $\phi' \approx 43°$ to $45°$. Using the NTH effective piezocone method of Senneset et al. (1989) in Fig. 7, an evaluation of the processed data from Figure 12 gives mean values for the cone resistance number $N_m = 18.3 \pm 2.5$ and pore pressure parameter $B_q = 0.56 \pm 0.07$. Assuming no adhesion and $\beta = 0$, the interpreted $\phi' \approx 46.4°$. While some might question the reasonableness of these values, high frictional parameters in triaxial compression have been observed for Mexico City clay with $\phi' \approx 43°$ (Diaz-Rodriguez, et. al. 1992) and Bothkennar clay with $37° < \phi' < 45°$ (Smith, et al. 1992).

Table 1. Index properties of Cooper Marl, South Carolina

Index	Mean	Range
water content, w_n	46.9	35 - 66
liquid limit, LL	82.9	60 - 129
plasticity index, PI	51.5	37 - 80
void ratio, e_0	1.27	0.93 - 1.66
percent fines, PF	66.8	42 - 93
clay fraction, CF	12.4	5 - 22
yield stress, σ_p' (kPa)	682	616 - 785
shear wave, V_s (m/s)	440	384 - 555

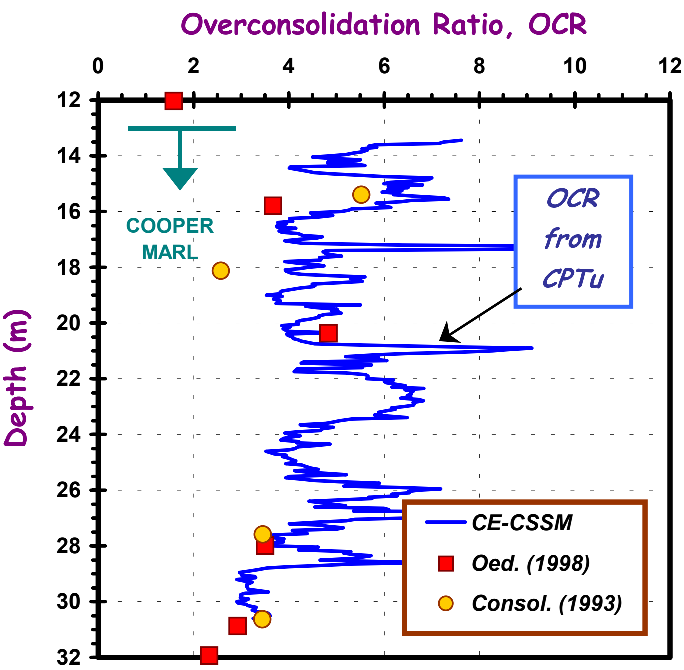

Figure 13. Measured and Predicted OCRs for Cooper Marl in Charleston, South Carolina, USA.

The SCE-CSSM approach has been used to evaluate the profile of overconsolidation ratio in the Cooper Marl per equation (15) with $\phi' = 43°$ and $\Lambda = 0.8$. The summary results shown in Figure 13 indicate good agreement with two different sets of consolidation tests performed on recovered tube samples.

Empirical estimates of the preconsolidation stress can also be made directly, yet these are dependent upon the plasticity and mineralogy of the clay, as well as other likely factors such as age, degree of fissuring, and sensitivity. For piezocone tests, a variety of parameters for obtaining σ_p' has been explored (Larsson & Mulabdić, 1991b). One such trend for a large database is presented in Figure 14 using the net cone tip resistance.

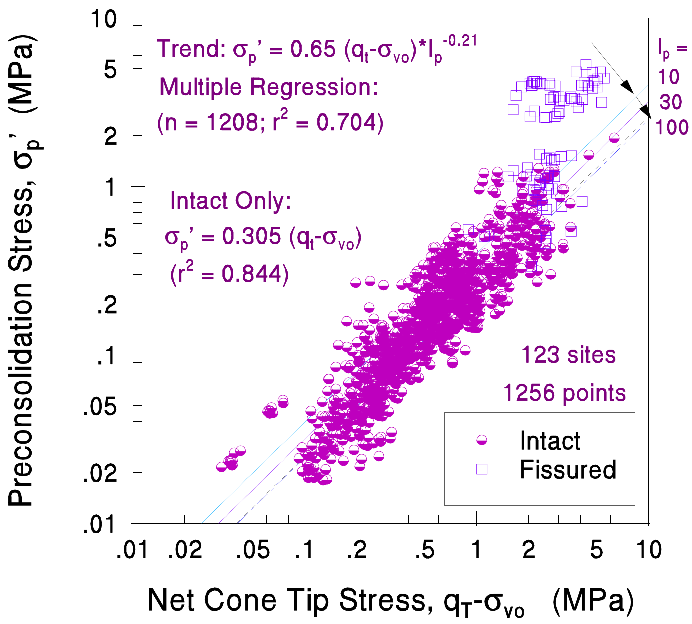

Figure 14. Empirical trend for σ_p' and net tip stress in clays. (After Chen & Mayne, 1996).

The mean trend from regression analysis on intact clays is given by:

$$\sigma_p' \approx 0.305\,(q_T - \sigma_{vo}) \tag{16}$$

It can be noted that the separate category of fissured geomaterials at high OCRs lies above this line, thus reflecting the added influence of the macrofabric of discontinuities on the penetration readings. In these cases, the preconsolidation stress will be under-estimated by (16).

The estimate for intact soils is improved if the clay plasticity index (PI or I_P) is considered. For type 2 cones, three trends can be realized from multiple regression analyses:

$$\sigma_p' \approx 0.65\,(q_T - \sigma_{vo})\,(I_P)^{-0.23} \tag{17}$$

$$\sigma_p' \approx 0.94\,(u_2 - u_o)\,(I_P)^{-0.20} \tag{18}$$

$$\sigma_p' \approx (q_T - u_2)\,(I_P)^{-0.18} \tag{19}$$

The ratio $\sigma_p'/(q_T-\sigma_{vo})$ does not uniquely decrease with plasticity index, however, as the organic clays of Sweden appear to show a more rapid rate of decrease with I_P than Japanese marine clays (Mayne, Robertson, & Lunne, 1998). The trends given by (17) through (19) thus do not include effects of geologic origin, organic content, and mineralogy.

These empirical correlations are nevertheless useful in providing an approximate check on the data and indication of reasonableness, as well as warning of

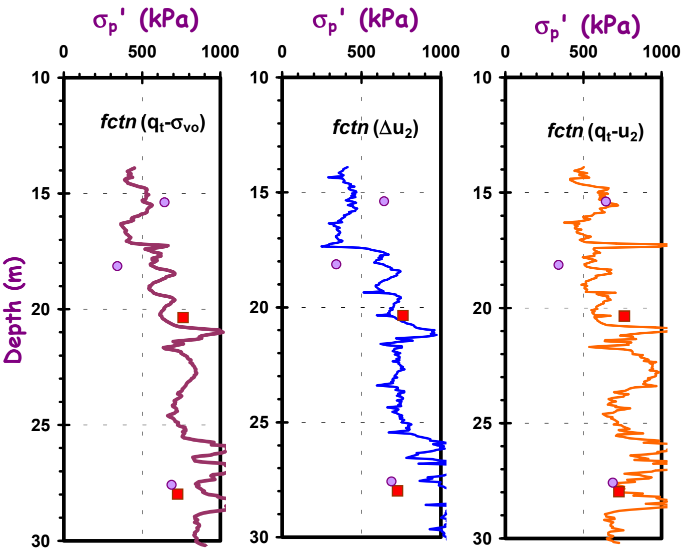

Figure 15. Empirical estimates of preconsolidation for the Cooper marl from piezocone correlations with plasticity index

anomalous behavior. For Cooper marl, the applications are shown in Figure 15 using an average $I_P = 52$.

3.2 *Dilatometer evaluation of OCR in clays*

Although the geometry of the flat plate dilatometer is non-axisymmetric, lab chamber experiments by Huang (1991) have shown excess porewater pressures generated in clays are essentially symmetric early on, just after installation of the blade. The observed magnitudes of Δu become directional later as dissipation occurs. Since the p_0 and p_1 readings are taken fairly early (within 15 to 45 seconds of penetration, respectively), cavity expansion can be used to approximate the level of induced pressures.

The contact pressures of the DMT are noted to be dominated by current porewater pressures (Mayne & Bachus, 1989). An analytical formulation using cylindrical cavity expansion and undrained strength from critical-state theory gives:

$$OCR = 2\left[\frac{2K_D}{(M \cdot lnI_R)}\right]^{1/\Lambda} \tag{20}$$

The evaluations of OCR with lateral stress index (K_D) and its possible variations with ϕ' and rigidity index (I_R) are evidenced in Figure 16. For this case, the analysis considers that passive failure may occur at high OCRs with the likely manifestations that a network of cracks and fissures are propagated in the soil mass. The limiting OCR can be estimated from a K_0-OCR relationship when K_0 reaches the passive stress coefficient (K_p), as discussed subsequently. At higher OCRs, then the operational undrained strength is reduced by a factor of two.

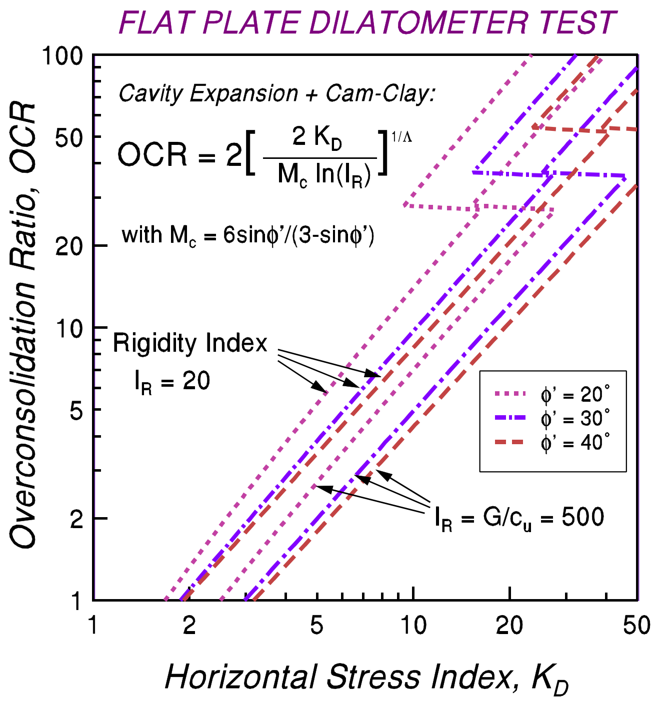

Figure 16. Cavity expansion-critical state relationships for OCR in terms of dilatometer K_D, rigidity index I_R, and ϕ' for clays.

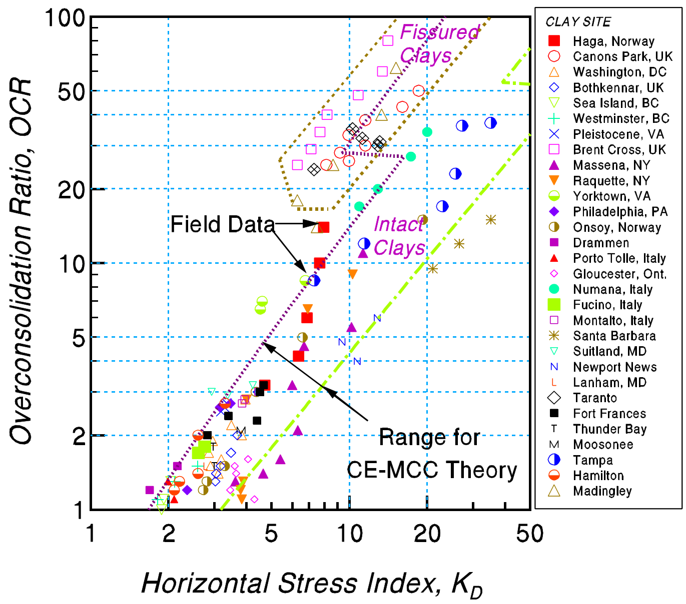

Figure 17. Calibration of OCR-K_D expression with DMT data.

The data tend to confirm the generalized relationship between OCR and K_D, including the effect of the fissuring macrofabric at high OCRs. In the aforementioned discussion of piezocone profiling, perhaps the negative porewater pressures observed in fissured materials already takes these effects into account. An alternative empirical approach for a quick evaluation of stress history in intact clays is (Mayne, 1995):

$$\sigma_p' \approx 0.51\ (p_0 - u_0) \tag{21}$$

4 INITIAL STRESS STATE

The initial state of stress is represented by the lateral stress coefficient, $K_0 = \sigma_{ho}'/\sigma_{vo}'$ and remains one of the most difficult parameters to measure accurately by either lab or field tests. Instead, for soils that have experienced a simple stress history caused by load-unloading, the following provides an estimate:

$$K_0 = (1-\sin\phi')\ OCR^{\sin\phi'} \qquad (22)$$

This expression was developed on the basis of instrumented oedometer tests, special triaxial stress-path tests, and other laboratory devices on clays, silts, sands, and gravels (Mayne & Kulhawy, 1982). More recently, field calibration by push-in spade cells, self-boring pressuremeter, and hydraulic fracturing tests have been carried out in clays, as summarized in Figure 18 (data compiled by Lunne, et al. 1990). For sands, the difficulty in sampling restricts the usual determination of associated preconsolidation, however, for a few well-characterized sands, Figure 19 appears to confirm that K_0 increases with OCR by field PMT.

Eventually, during unloading, the value of K_0 increases to reach the passive failure state. If a conservative Rankine criterion is adopted, then the maximum lateral stress state is given by:

$$K_p = (1+\sin\phi')/(1-\sin\phi') \qquad (23)$$

When (22) is equated to (23), a limiting OCR can be given by:

$$OCR_{limit} \approx [(1+\sin\phi')/(1-\sin\phi')^2]^{1/\sin\phi'} \qquad (24)$$

The limiting OCR can be greater than allowed by (24) if a proper assessment of the effective cohesion intercept (c′) is taken into account. Many triaxial tests over a wide range of stresses and different stress paths are needed to define the yield surface, however. The generalized expression for K_p is then:

$$K_p = \frac{1+\sin\phi'}{1-\sin\phi'} + (2c'/\sigma_{vo}')\sqrt{\frac{1+\sin\phi'}{1-\sin\phi'}} \qquad (25$$

The relevant value of c′ appears to be controlled by rate effects, age, test mode, and other factors. It is also the intercept of a forced fit of a linear Mohr-Coulomb criterion to a curved yield surface, and thus depends on stress level (Mesri & Abdel-Ghaffar, 1994). In this case, the following is recommended for estimating short-term situations:

$$0.02 < (c'/\sigma_p') < 0.04 \qquad (26)$$

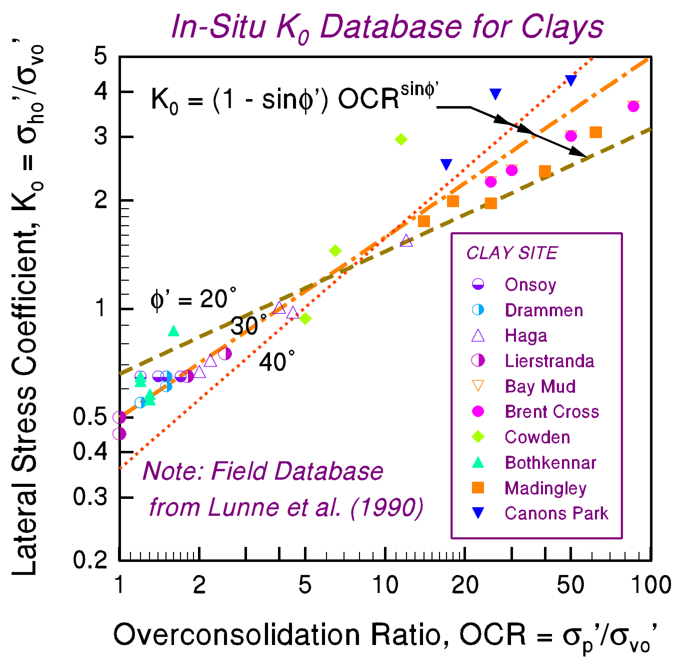

Figure 18. Field data from K_0 measurements in clays. (Data compiled by Lunne et. al., 1990).

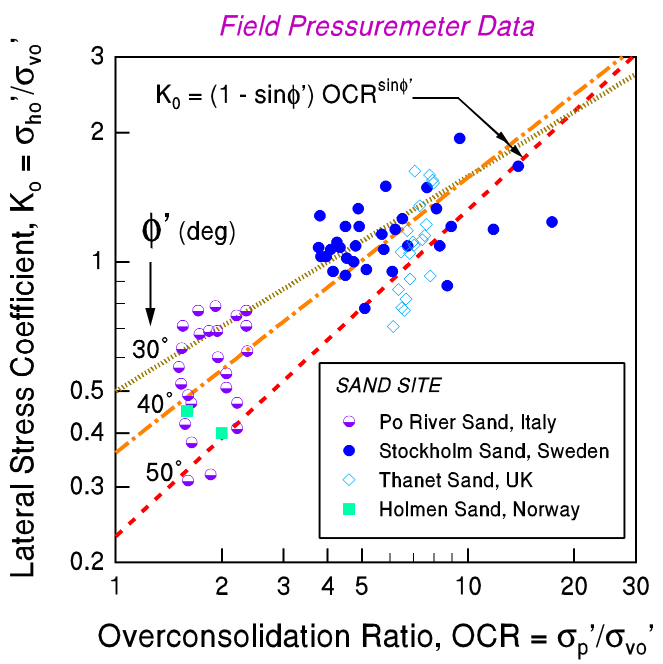

Figure 19. Field data from PMT K_0 measurements in sands.

4.1 *Geostatic stress state of clays*

Although correlations for estimating K_0 in clays are possible from the DMT K_D index (e.g., Marchetti, 1980) or CPTu parameters (e.g., Mayne & Kulhawy, 1990), a more consistent approach is achieved by first assessing the OCR and then using (22) for clays prestressed by mechanical overconsolidation. Notably, more research is still needed in quantifying the magnitudes of K_0 caused by desiccation, aging, cyclic loading, and cementation.

4.2 *Geostatic stress state and OCR of sands*

The in-situ K_0 in sands may be assessed indirectly by in-situ penetration tests such as the DMT, as discussed elsewhere (e.g., Schmertmann, 1986; Mayne & Martin, 1998). For the CPT, a statistical evaluation of a large database (n = 590) compiled from 26 separate series of calibration chamber tests has produced the empirical relationship shown in Figure 20 for both NC and OC sands. If the expression for effective horizontal stress is normalized by the effective vertical stress, the relevant K_0 can be expressed by the following regression equation ($r^2 = 0.871$):

$$K_0 = 1.33(q_T)^{0.22} (\sigma_{vo}')^{-0.31} OCR^{0.27} \quad (27)$$

where q_T is in MPa and σ_{vo}' in kPa. Of course, the formulation applies only to unaged and uncemented quartzitic sands and has been verified by a limited number of field test sites (Mayne, 1995b). If an assumed K_0 - OCR relationship is assumed apriori, it might take the general form:

$$K_0 = K_{0NC}\, OCR^{\alpha} \quad (28)$$

Solving (27) and (28) provides the following direct solution for OCR:

$$OCR = \left[\frac{1.33}{K_{0NC}} \frac{q_T^{\,0.22}}{(\sigma_{vo}')^{0.31}}\right]^{1/(\alpha - 0.27)} \quad (29)$$

If (22) is an estimator for (28), then $K_{0NC} = (1\text{-}\sin\phi')$ and $\alpha = \sin\phi'$. The profile of OCR (and associated K_0 values) can be then be obtained directly with depth.

An example use of (29) is given in Figure 21 for Stockholm sand (Dahlberg, 1974). Originally, a 24-m thick deposit of glacial sand was available that was subsequently quarried for construction use. After 16 m of excavation, a large test program employing many different types of in-situ tests was conducted, including SPT, CPT, PMT, screw plate tests, inplace densities, as well as laboratory testing.

In the original citation, the deduced profile of OCR was ascertained by calculation of the mechanical overburden removed: $OCR = (\Delta\sigma_v + \sigma_{vo}')/\sigma_{vo}'$ that was verified with preconsolidation stresses interpreted from screw plate tests. In addition, the corresponding K_0 profile was assessed and agreed with lift-off pressures from PMTs.. Figure 21 shows the CPT approach applied to Stockholm obtained using (3) to obtain ϕ' with depth ($\phi' \approx 40° \pm$) and (29) to generate the OCR profiles from two nearby soundings.

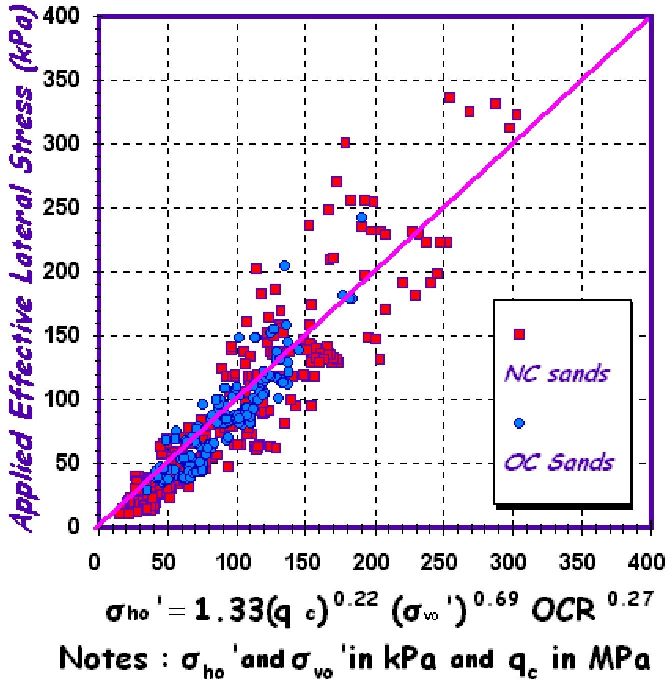

Figure 20. CPT calibration chamber relationship for evaluating teral stresses in unaged clean quartz sands.

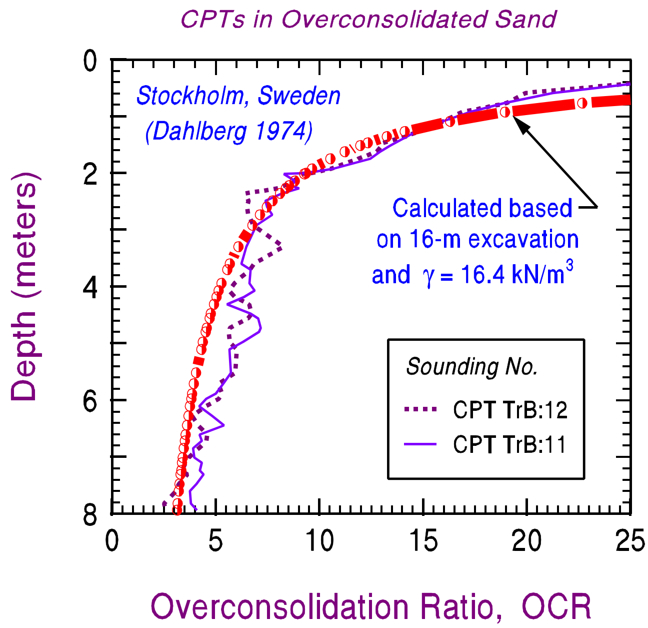

Figure 21. CPT-evaluated profile of OCR in Stockholm sand deposit (data reported by Dahlberg, 1974).

Of recent, the use of paired (or more) sets of directional shear wave velocity measurements have been explored for deciphering the in-situ geostatic state of stress in soils and further work in this direction will be interesting (e.g., Fioravante, et al. 1998; Sully & Campanella, 1995). The downhole V_s from SCPT and SDMT provides at least one vertically-directed profile and could be coupled with data from surface SASW series (e.g., Butcher & Powell, 1995).

5 DEFORMATION PARAMETERS

The deformation characteristics of soils include the consolidation indices (C_c, C_s, C_r) and elastic moduli (E, G, K, B), as well as rate and creep parameters. The discussions herein will focus on elastic parameters to represent soil stiffness under monotonic loading. The stiffness of soils is needed in evaluating deflections of shallow & deep foundations, retaining walls, and excavations, and embankments. Stiffness can be measured in-situ using the pressuremeter, plate load test, dilatometer, screw plate, and geophysical methods, albeit these all provide moduli at different points along the stress-strain curve.

With the recent interest in enhanced in-situ testing for geotechnical site characterization, it is timely to discuss the use of seismic piezocone (SCPTu) and dilatometer (SDMT) for the evaluation of stiffness over a range of stress-strain-strength responses, since data are collected at two opposite ends of the curve. A modified hyperbola (Fahey & Carter, 1993) can be used to conveniently degrade the initial stiffness (E_0) with increasing load level and provide nonlinear load-displacement-capacity results.

Despite the repeated attempts to estimate deformation parameters from routine penetration test data, the stiffness of soils is not really well-represented at the peak resistances that occur at failure strains or beyond (Figure 22). In fact, most of the activity of interest in earthwork deformations takes place close to the in-situ K_0 state and corresponding small-strain region characterized by G_{max} (Burland, 1989).

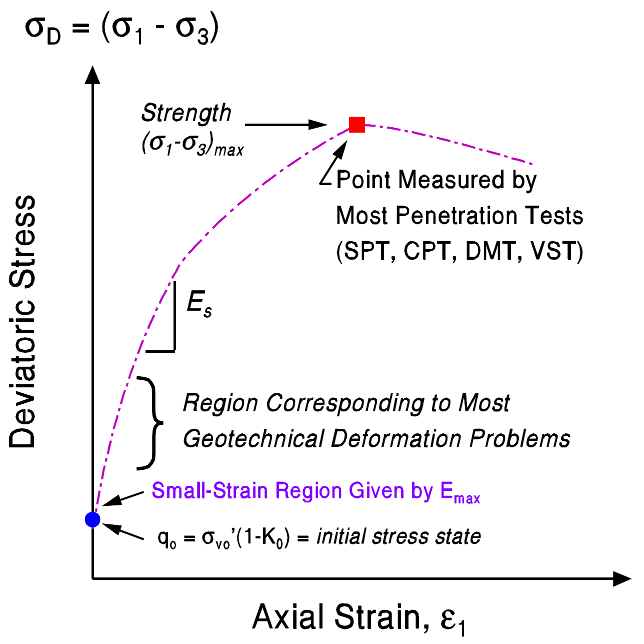

Figure 22. Conceptual stress-strain response of soils

5.1 *Small-strain stiffness*

Recent research has found that the small-strain stiffness from shear wave velocity (V_s) measurements applies to the initial static monotonic loading, as well as the dynamic loading of geomaterials (Tatsuoka & Shibuya, 1992; Jardine, et al., 1991). Thus, the original dynamic shear modulus (G_{dyn}) has been re-termed the maximum shear modulus (designated G_{max}), or alternatively, the small-strain shear modulus (G_0), that provides an upper limit stiffness given by:

$$G_0 = \rho_T V_s^2 \tag{30}$$

where $\rho_T = \gamma_{T/}g$ = total mass density, γ_T = soil unit weight, and $g = 9.8$ m/s^2 = gravitational constant. The modulus G_0 is a fundamental stiffness of all solids in civil engineering and can be measured in all soil types from colloids, clays, silts, sands, gravels, to boulders and fractured rocks. Interestingly, G_0 applies to drained and undrained soil behavior, because at such small strains, porewater pressures have not yet been generated. The concept of a threshold strain would mark the onset of Δu. The corresponding equivalent elastic Young's modulus is found from:

$$E_0 = 2G_0\,(1+\nu) \tag{31}$$

where $0.1 \leq \nu \leq 0.2$ is the appropriate range of values for Poisson's ratio of geomaterials at small strains.

5.2 *Shear wave measurements*

The shear wave velocity can be measured in conventional cased boreholes using the crosshole test (CHT) and downhole test (DHT), or with improved surface techniques such as spectral analysis of surface waves (SASW), seismic refraction (SR), and reflection surveys. Also available is the suspension logger and downhole methods of SCPTu and SDMT. The latter are convenient in that they can map the geostratigraphic profiles, strength characteristics, and obtain a DH measurement of V_s within the same sounding.

A representative SCPTu (one of 15) obtained in soft varved clay at the National Geotechnical Experimentation Site (NGES) in Amherst, MA is shown in Figure 23. A companion SDMT at the same site has been presented elsewhere (Mayne, et al. 1999a). The site profile consists of 1 m of clay fill over a 3-m desiccated clay crust, underlain by varved lacustrine silty clay. Groundwater lies 1 m deep. High excess porewater readings are evidence of clay materials. The procedure of individual rod breaks at 1-m intervals can be noted here as well.

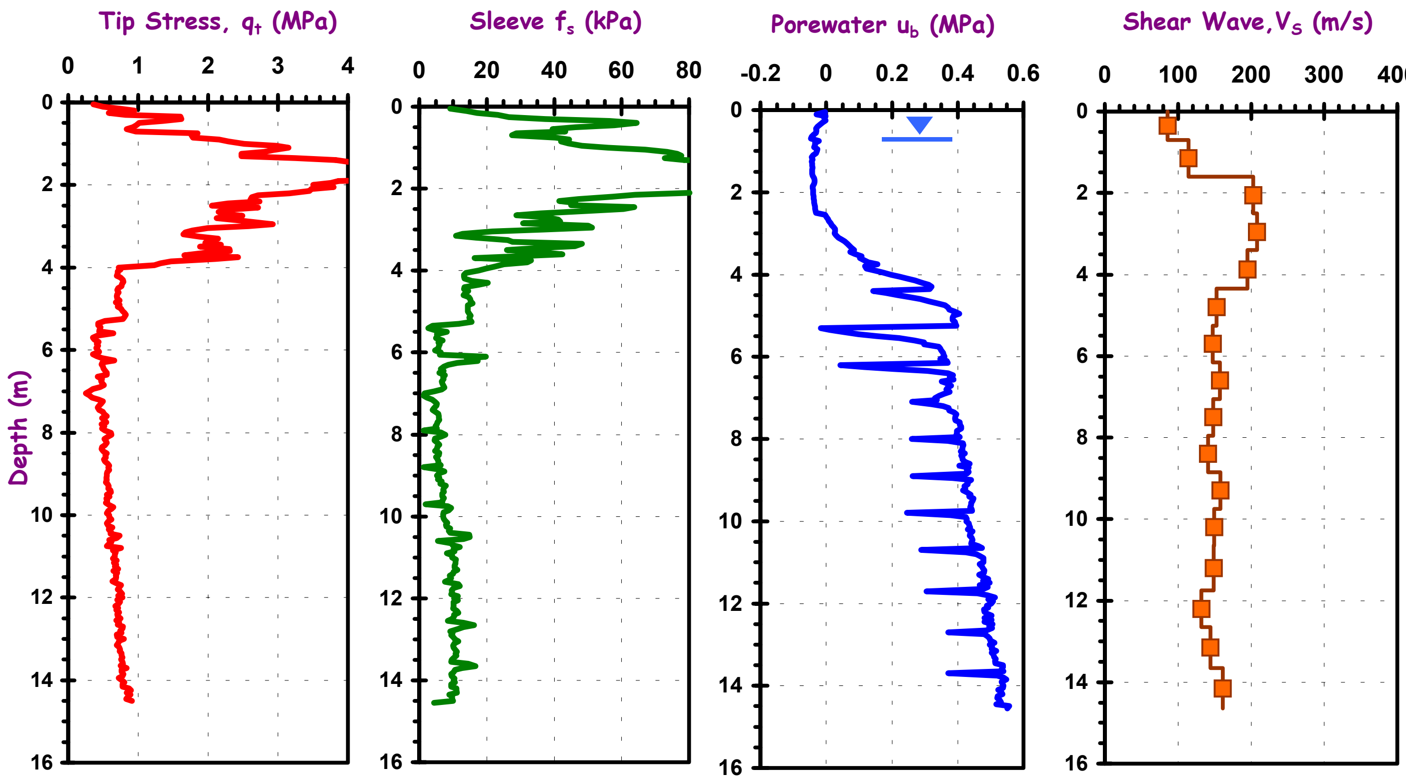

Fgure 23. Respresentative seismic piezocone results in varved clay at NGES in Amherst, Massachusetts.

In order to obtain the initial stiffness G_{max}, an estimate or measurement of mass density or unit weight is needed. A global compilation of V_S data from all types of saturated geomaterials ranging from clays to gravels to rocks finds the the following trend:

$$\gamma(\text{sat}) = 8.32 \log V_S - 1.61 \log z \qquad (32)$$

where γ(sat) is in kN/m^3, V_S (m/s),and z (meters). The estimate is also handy for calculating σ_{vo} and σ_{vo}'.

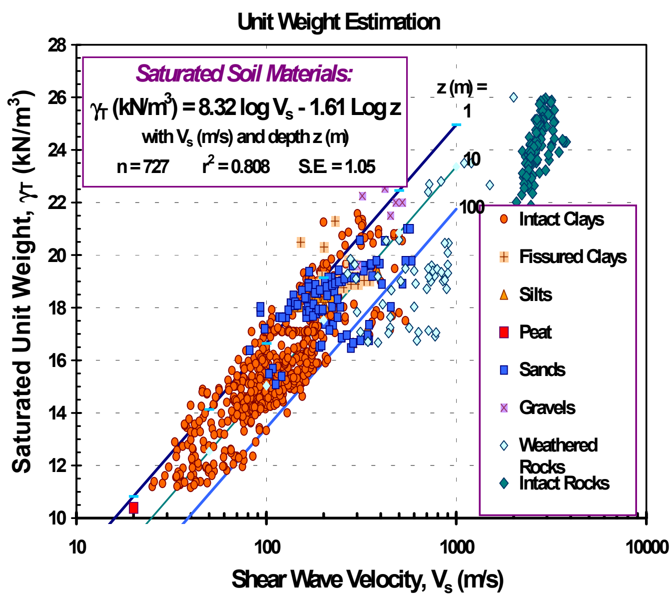

Figure 24. Correlation for unit weight from depth and V_S.

5.3 *Intermediate stiffness of soils*

The stress-strain-strength-time response of soils is complex, highly nonlinear, and depends upon loading direction, anisotropy, rate effects, stress level, strain history, time effects, and other factors. It is therefore a difficult issue to recommend a single test, or even a suite of tests, that directly obtains the relevant E_s for all possible types of analyses in every soil type. This is because the modulus varies considerably with strain level (or stress level).

In certain geologic settings and types of geomaterials, it has in fact been possible to develop calibrated correlations between specific tests (e.g., PMT, DMT) with performance monitored data obtained from full-scale structures, including foundations and embankments, or with reference values from laboratory test. These tests will provide a modulus somewhere along the stress-strain-strength curve (Fig. 25), generally at an intermediate level of strain. Of particular note, the small-strain modulus from shear wave velocity measurements provides an excellent reference value, as this is the maximum stiffness that the soil can exhibit at a given void ratio and effective confining state. Herein, a generalized approach based on the small strain stiffness from shear wave measurements will be discussed, whereby the initial modulus (E_0) is degraded to an appropriate stress level, or current factor of safety (FS).

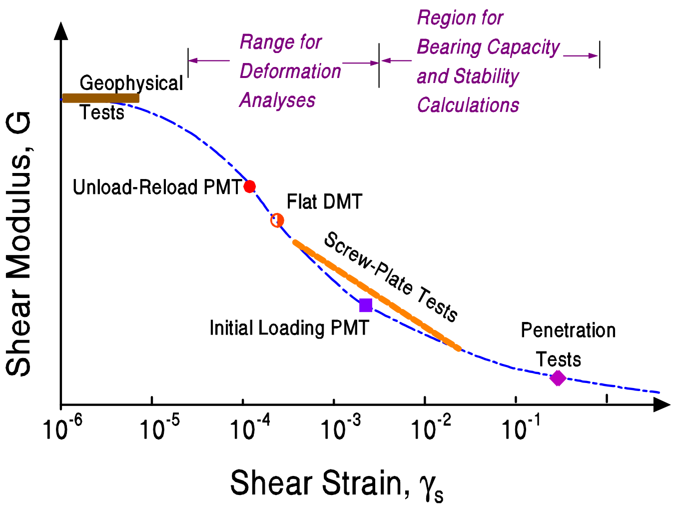

Figure 25. Reduction of shear modulus with level of strain.

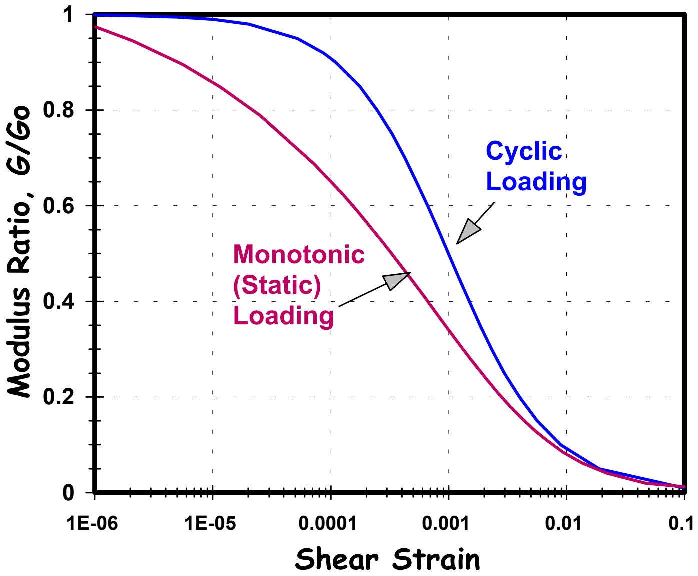

Figure 26. Modulus reduction for monotonic & cyclic loading

The shear modulus decreases with shear strain level and is commonly shown in normalized form, with current G divided by the maximum G_{max} (or G_0). The relationship between G/G_0 and logarithm of shear strain is well recognized for dynamic loading conditions (e.g., Vucetic and Dobry, 1991), however, the monotonic static loading curves show a more rapid decay with strain, as depicted in Figure 26. The cyclic response is representative of data obtained from laboratory resonant column tests, whereas the monotonic curve has been only more recently addressed with the advent of special internal & local strain measurements in triaxial tests, as well as by torsional shear devices (Jamiolkowski, et al. 1994).

Laboratory monotonic shear tests with high-resolution deformation instrumentation have shown that strain data obtained external to the triaxial cells are flawed because of seating errors, bedding problems with the filter stone, and boundary effects at the specimen ends. Thus, old strain data show geomaterials generally softer than they really are. New internal measurements are now available that accurately measure the soil stiffness at small- to intermediate- to large-strains (LoPresti, et al. 1993, 1995; Tatsuoka & Shibuya, 1992). Figure 27 shows a selection of normalized secant moduli (E/E_0) at their corresponding mobilized stress level (q/q_{ult}) obtained from lab tests on uncemented and unstructured geomaterials.

5.4 *Stress-strain-strength representation*

A modified hyperbola can be used as a simple means to reduce the small-strain stiffness (E_0) to secant values of E at working load levels, in terms of the mobilized strength (q/q_{ult}). Figure 28 illustrates the representative modulus reduction scheme for unstructured clays and uncemented sands. The generalized form may be given as (Fahey & Carter, 1993; Fahey et al. 1994):

$$E/E_0 = 1 - f\,(q/q_{ult})^g \qquad (33)$$

where f and g are fitting parameters. Values of $f = 1$ and $g = 0.3$ appear reasonable first-order estimates for unstructured and uncemented geomaterials (Mayne, et al. 1999a) and these provide a general fit for the data shown in Figure 27. The mobilized stress level can

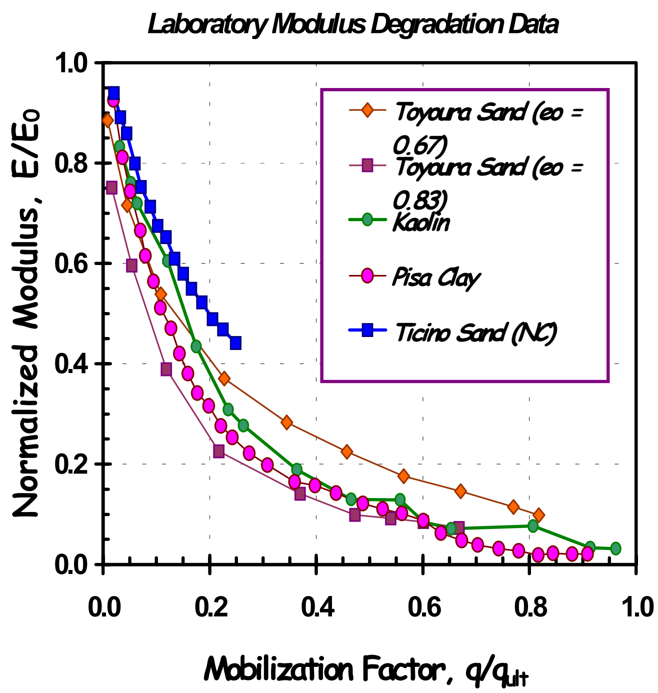

Figure 27. Modulus degradation in terms of mobilized stress from instrumented laboratory test specimens.

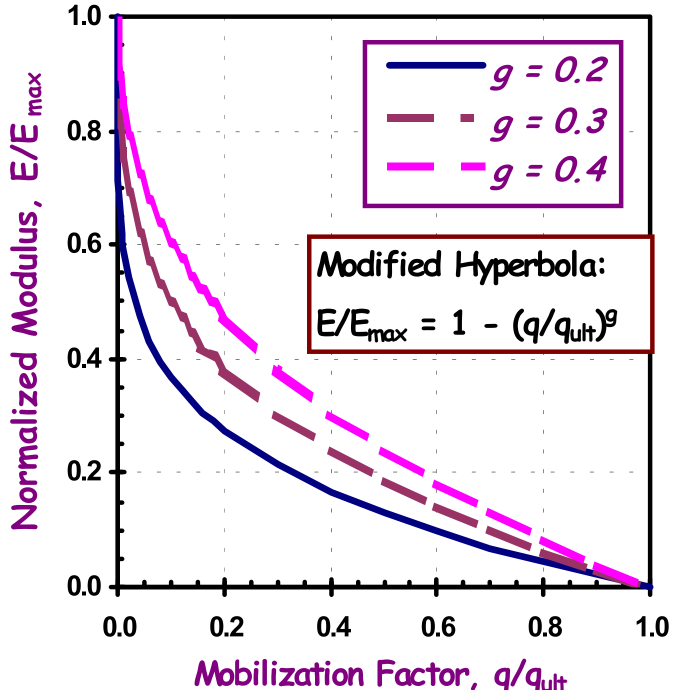

Figure 28. Modified hyperbolic curves to represent modulus reduction from small-strain region to intermediate strains.

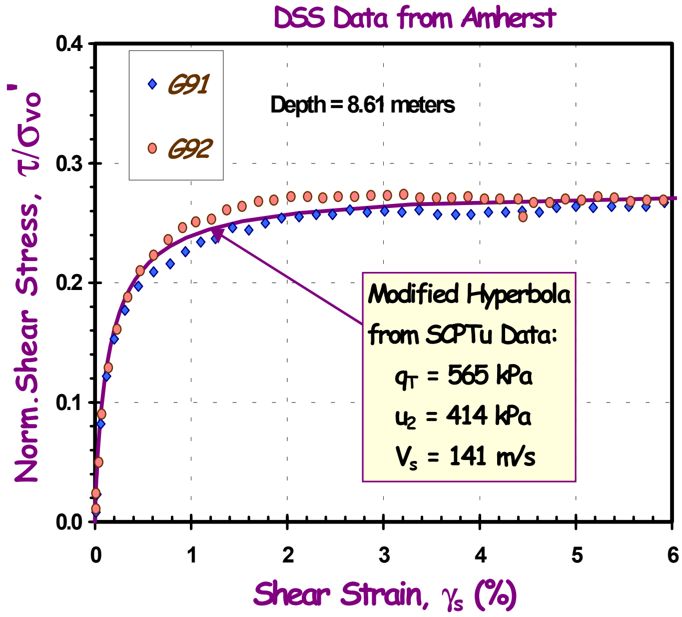

Figure 29. Applied modified hyperbola to SCPTu data and comparison with laboratory DSS data on Amherst soft clay.

also be considered as an inverse factor of safety, or $(q/q_{ult}) = 1/FS$. That is, for a stress level half of ultimate, $(q/q_{ult}) = 0.5$ and the corresponding FS = 2.

Modulus reduction has been addressed using a number of different numerical schemes (e.g., Duncan & Chang, 1970; Hardin & Drnevich, 1972; Prevost & Keane, 1990; Tatsuoka & Shibuya, 1992). Several of these approaches have a more fundamental basis or a better fitting algorithm over the full range of strains from small- to intermediate- to large-ranges (e.g., Puzrin & Burland, 1996, 1998). Herein, only an approximate approach has been sought so that the V_S data may be incorporated into stress-strain estimations, starting from the initial stiffness and quickly reducing these values to intermediate- and high-strain regions of soil stiffness.

From the SCPTu field data in soft Amherst clay given in Figure 23, the degree of overconsolidation and derived shear strengths for simple shear have been evaluated. The initial stiffness has been taken from the V_S data and a modified hyperbola used to connect the two ends of the curve. Measured results from two laboratory DSS tests (nos. G91 and G92) on specimens taken from the same depths are shown to be in nice agreement with the predicted curves in Figure 29. Since data are taken along the entire depth of the sounding, it is possible to generate nonlinear τ-γ_s curves for all depths, if desired. Illustrative stress-strain comparisons are made from SCPTu (Burns & Mayne, 1996) and SDMT data (Mayne, et al., 1999).

6 FLOW CHARACTERISTICS

The hydraulic conductivity (k) and coefficient of consolidation (c_v) represent the flow characteristics of fluids through the soil mass. In this regard, the excess porewater pressures generated during probe installation can be monitored with time at periodic stops in the sounding. Several methods of interpreting piezocone dissipation tests have been available for this purpose (e.g. Teh & Houlsby, 1991), however, prior derivations have been developed solely to address *monotonic* decay of porewater pressures with time. With type 2 penetrometers, a *dilatory* response can occur in overconsolidated fissured materials, whereby the porewater values initially increase during dissipation, reach a peak, and then subsequently decay with time. In addition, existing approaches only match a single point (usually 50%) of the recorded dissipation.

6.1 *CE-CSSM approach*

Using the hybrid cavity expansion-critical state formulation described earlier, the octahedral normal and shear-induced components can be allowed to dissipate separately. The summation of their responses given (Figure 30) provides the type of measured behavior during porewater dissipation. The octahedral component is obtained from (11) and always a positive value, whereas shear-induced values from (13) can be positive or negative depending upon the degree of OCR and frictional qualities. Moreover, the large octahedral zone will require long times to decay because of the noted soil volume influenced. In contrast, the shear zone occurs as a thin annulus that will decay more rapidly. It is possible, therefore, to represent both monotonic and dilatory responses with this approach. Full details are given elsewhere on the solving of the second-order differential equation for radial flow and consolidation (Burns & Mayne, 1998). Herein, only a brief review of the features will be discussed and an approximate closed-form given for practical use.

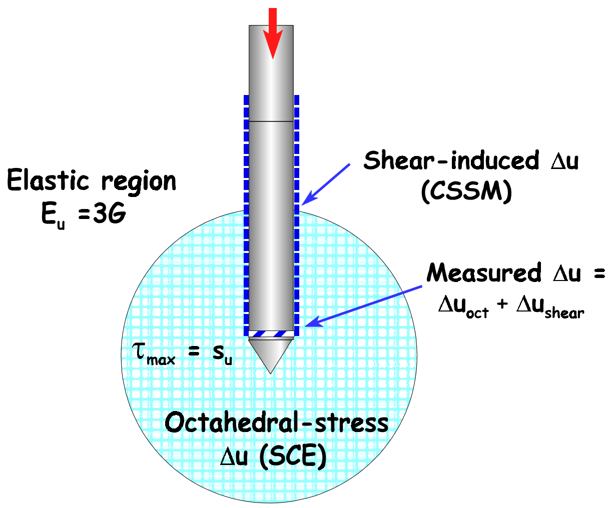

Figure 30. Normal- and shear-induced components of excess porewater pressures around the cone.

In lieu of merely matching one point on the dissipation curve (i.e, t_{50}), the entire curve is matched to provide the best overall value of the horizontal coefficient of consolidation (c_h). The excess porewater pressures Δu_t at any time t can be compared with the initial values during penetration (Δu_i). measured initial excess porewater pressure ($\Delta u_i = u_2 - u_o$) is given by:

$$\Delta u_i = (\Delta u_{oct})_i + (\Delta u_{shear})_i \quad (34)$$

where $(\Delta u_{oct})_i = (2/3)M\sigma_{vo}'(OCR/2)^{\Lambda} \ln I_R$ = the octahedral component during the penetration and $(\Delta u_{shear})_i = \sigma_{vo}'[1 - (OCR/2)^{\Lambda}]$ is the shear-induced component. For practical use, an approximate closed-form expression is presented here. The porewater pressures at any time (t) are obtained in terms of the modified time factor T* from:

$$\Delta u = \frac{(\Delta u_{oct})_i}{1 + 50T^*} + \frac{(\Delta u_{shear})_i}{1 + 5000T^*} \quad (35)$$

where the modified time factor is defined here by:

$$T^* = \frac{c_h\, t}{a^2\,(I_R)^{0.75}} \quad (36)$$

and a = probe radius. Using a spreadsheet, log values of T* are established and used to generate corresponding times t for given I_R and a. Trial & error is performed on the value of c_h to give the best fit.

6.1 *Monotonic Dissipations*

A representative look at monotonic dissipation is shown in Figure 31 for the Amherst site (z = 12.2 m). Using (35) and (36) with the following input parameters (OCR = 1.8, I_R = 227, ϕ' = 33°, Λ = 0.8), the predicted response is also indicated using a trial & error for the entire Δu recording with time to determine a best fit c_h = 0.5 cm^2/min.

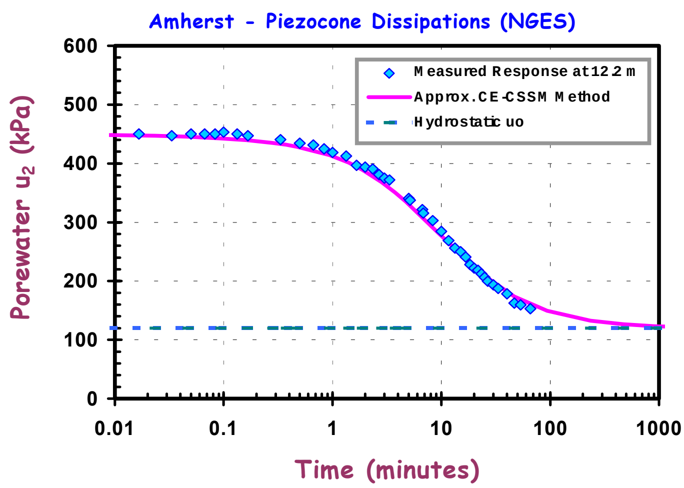

Figure 31. Measured and fitted montonic dissipations in soft clay at Amherst site (data from Lutenegger, 2000).

6.2. *Dilatory Dissipations*

In contrast, a dilatory type curve is shown in Figure 32 for the hard Taranto clay (data from Pane, et al. 1995). Here, the CE-CSSM model used the following input parameters (OCR = 28, I_R = 12, ϕ' = 28°, Λ = 0.8) to obtain the fit for c_h.

A summary comparison of measured c_v from laboratory oedometer and consolidation tests with the piezocone fitted c_h values using the rigorous method is presented in Figure 33. The categories include intact clays, desiccated crustal clays, and fissured materials. Curves showing normalized excess porewater pressures from the rigorous method for various OCR and ϕ' have also been given (Burns & Mayne, 1998).

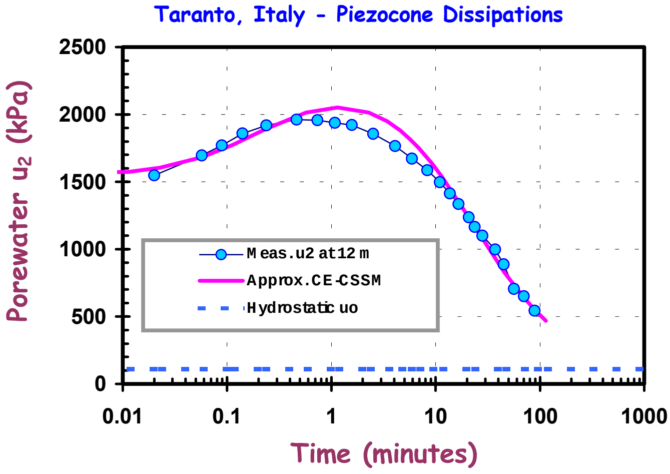

Figure 32. Measured and fitted dilatory response in the hard overconsolidated Taranto clay (data from Pane, et al. 1995).

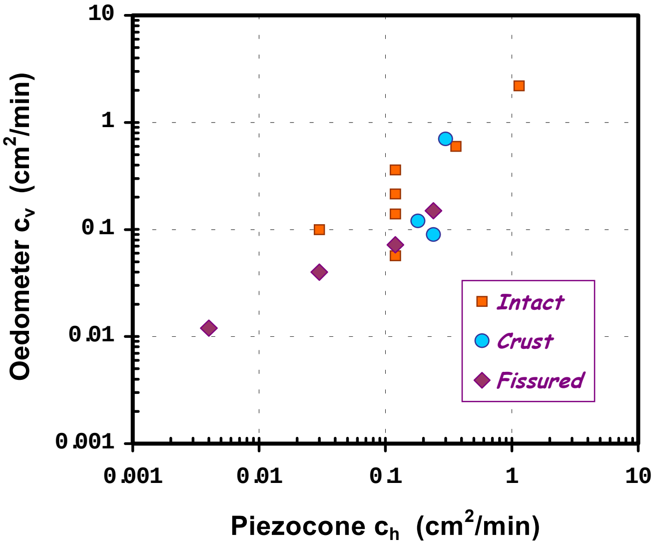

Figure 33. Comparison of consolidation coefficients from oedometer and piezocone for clays (Burns & Mayne, 1998).

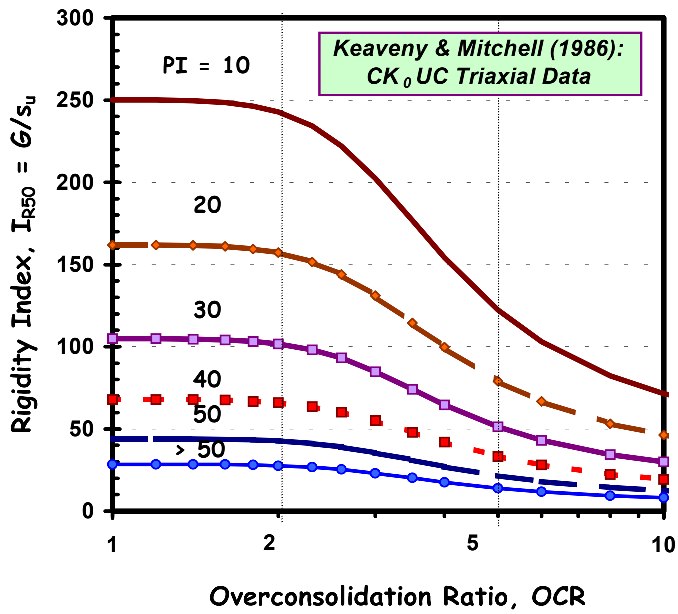

Figure 34. Empirical rigidity estimate from PI and OCR.

6.3 *Undrained Rigidity Index*

For the evaluation of c_h from piezocone dissipation tests using any of the cavity expansion or strain path methods, an evaluation of undrained rigidity index is required. If quality samples are available, the value of $I_R = G/s_u$ can be assess at 50% of the peak strength. Results from pressuremeter tests (PMT) can also be used. In many cases, the site exploration may solely rely on soil borings with SPTs and companions series of CPTs. Thus, some direction towards the evaluation of I_R is warranted.

An empirical approach between $I_{R,}$ OCR, and PI has been published on the basis of CAUC triaxial test data (Keaveny & Mitchell, 1986). Figure 34 presents the empirical curves that show $I_{R,}$ decreasing with OCR and PI which may approximately be expressed by:

$$I_R \approx \frac{\exp\left(\frac{137-I_P}{23}\right)}{1+\ln\left[1+\frac{(OCR+1)^{3.2}}{26}\right]^{0.8}} \tag{37}$$

Alternatively, a Cam-clay derivation has been suggested that depends on routine soil parameters for input (Kulhawy & Mayne, 1990). Figure 35 illustrates the curves obtained by this approach ($\Lambda = 0.8$) which can be calculated from:

$$I_R = \left(\tfrac{2}{3}\right)\, M\, \frac{1+e_0}{C_c}\, \ln(10)\frac{[1+\ln(OCR)]\exp(\Lambda)}{\Lambda(1-\Lambda)OCR^{\Lambda}} \tag{38}$$

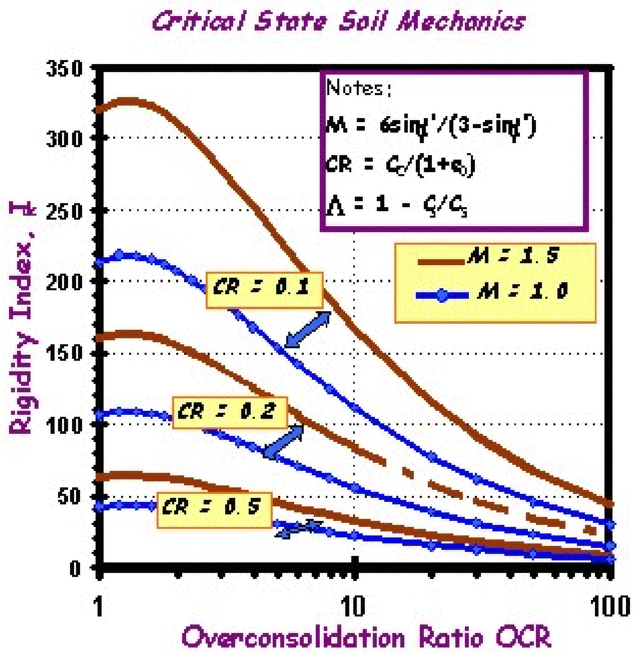

Figure 35. Rigidity index from Cam-clay derivation.

The third and final method discussed is a reformulation of the SCE-CSSM method for piezocone penetration. Interestingly, the backcalculation of soil rigidity index ($I_R = G/s_u$) from (9) is accomplished using (7) and (15) to provide a direct evaluation as:

$$I_R = \exp\left[\left(\frac{1.5}{M} + 2.925\right)\left(\frac{q_t - \sigma_{vo}}{q_t - u_2}\right) - 2.925\right] \qquad (39)$$

The expression is somewhat sensitive to the quality of input data because of the exponential form, thus the importance in using class 3 penetrometers (Lunne, et al., 1997) for this purpose. An example evaluation using piezocone data from the UK test site at Bothkennar, Scotland is presented below in Figure 36. The profile compares well with the aforementioned empirical approach using PI and OCR that give good estimates of c_h.

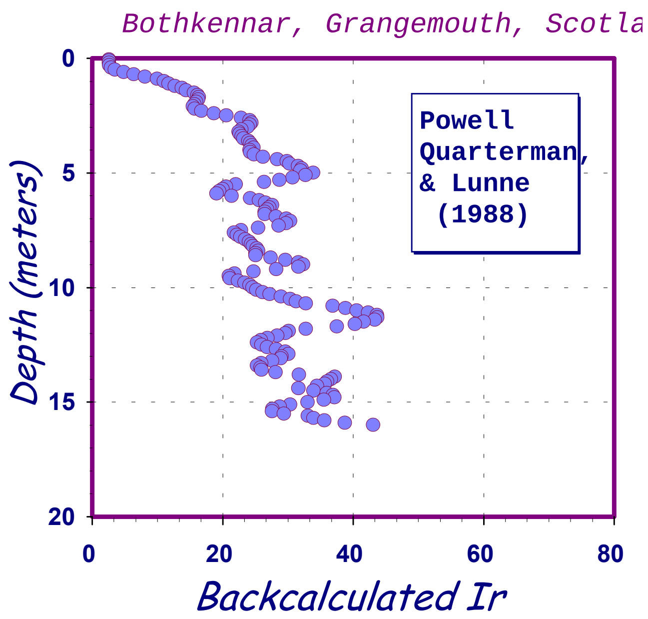

Figure 36. Direct rigidity index from CPTu measurements.

6.4 *Permeability*

Once the coefficient of consolidation has been determined, the hydraulic conductivity or permeability (k) can be evaluated from:

$$k = c_h\, \gamma_w / D' \qquad (40)$$

where $D' = 1/m_v$ = constrained modulus, as defined from one-dimensional oedometer tests and $\gamma_w = 9.8$ kN/m^3 = unit weight of water. In lieu of a direct measure of D', it seems possible that this stiffness might correlate with the small-strain modulus from shear wave velocity measurements. As such, Figure 37 presents a compiled database on clays where both laboratory consolidation moduli (D') and field values of G_0 were available. A conservative trend appears to be defined by:

$$D' = 0.1\, G_0 \qquad (41)$$

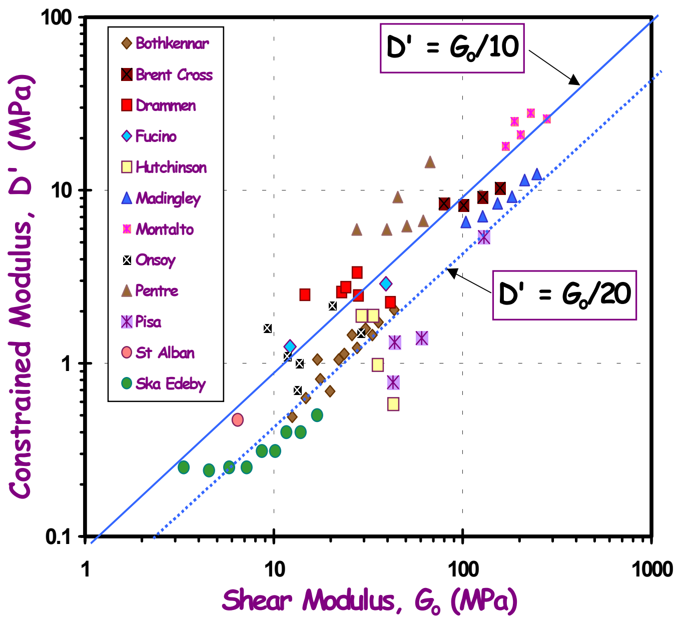

Figure 37. Relationship for constrained modulus from small-strain shear modulus in clays.

Alternatively, a first-order estimate on the constrained modulus is obtained from the net tip resistance (Kulhawy & Mayne, 1990):

$$D' = 8.25\,(q_T - \sigma_{vo}) \qquad (42)$$

Using the aforementioned value $c_h = 0.5$ cm^2/s for z = 12.2 m at the Amherst site and the SCPTu data from Figure 23 ($q_T = 690$ kPa; $V_S = 140$ m/s), the evaluated parameters are $\gamma_T = 16.1$ kN/m^3, $G_{max} = 32.2$ MPa, and $D' = 3.2$ MPa (per eqn 41), giving a permeability $k = 2.53 \cdot 10^{-7}$ cm/s. This corresponds well to the reported value from laboratory testing (and other field methods) of $k = 4 \cdot 10^{-7}$ cm/s at z = 12.2 m given by DeGroot & Lutenegger (1994).

As a check, an empirical estimate of k can be made directly from the t_{50} reading(Parez & Fauriel, 1988). This is conveniently approximated by:

$$k\ (\text{cm/s}) = (251 \cdot t_{50})^{-1.25} \qquad (43)$$

where t_{50} is in seconds (Finke & Mayne, 2001). For $t_{50} = 600$ s scaled from Fig. 31, (43) provides another reasonable estimate of $k = 3.37 \cdot 10^{-7}$ cm/s.

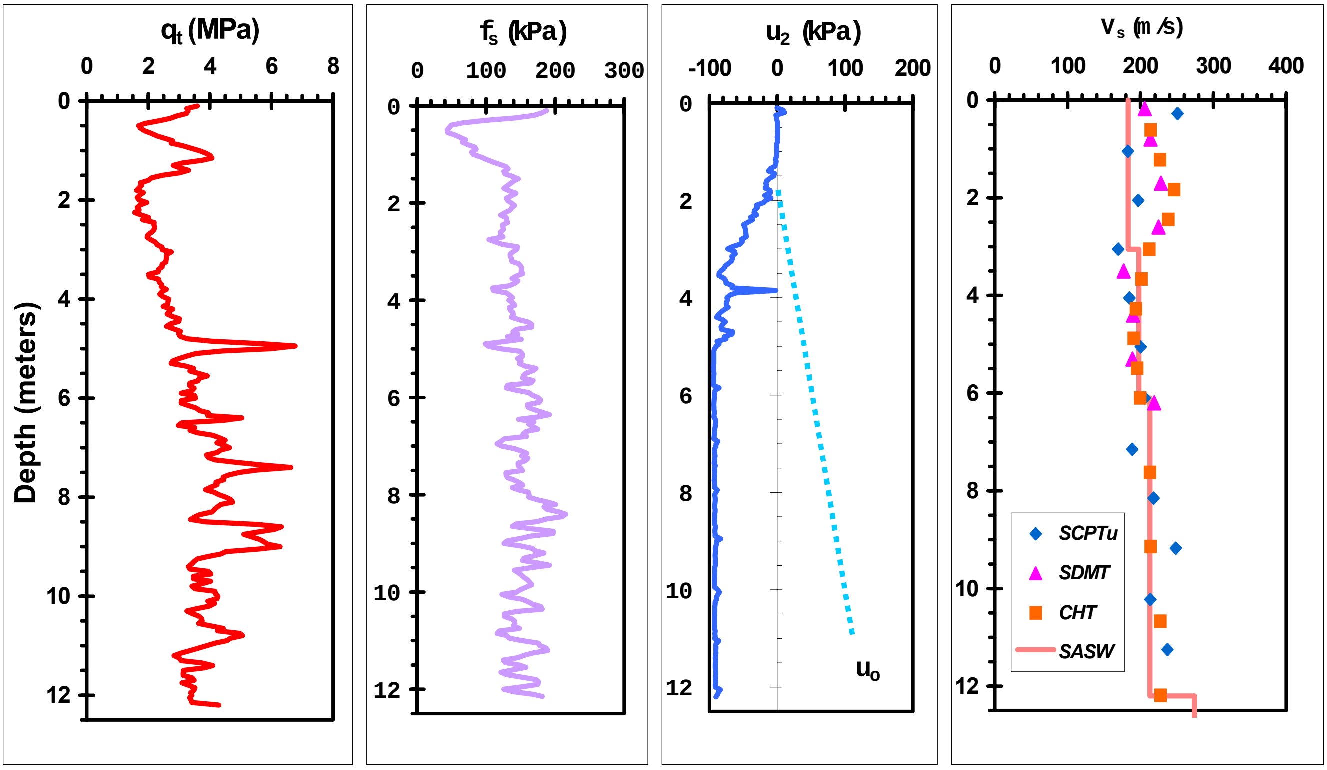

Figure 38. Results of seismic piezocone tests in residuum at Opelika NGES, Alabama, USA (Schneider, et al., 1999).

7 DIRECT APPLICATIONS

Another approach to utilization of SCPTu and SDMT data is the direct application of the measured resistances to foundation analyses (e.g., Robertson, et al., 1988). Along these lines, full-scale load tests from the new National Geotechnical Experimentation Site (NGES) at Opelika, Alabama will be presented. A drilled shaft was constructed under slurry installation methods with a diameter d = 0.914 m and embedded length L = 11.0 m. The soil profile consists of residual soils (ML and SM) of the Piedmont geology derived from the inplace weathering of metamorphic and igneous rocks, primarily schist, gneiss, and granites.

Results from a representative seismic piezocone sounding at the site are shown in Figure 38. The negative porewater pressures are typical in this geology (Finke & Mayne, 2001). The downhole shear waves from CHT, DHT, and SASW compare well (Schneider et al., 1999). At this site, the DHT values were obtained using both series of seismic cone and seismic dilatometer tests.

The side friction component was calculated on the basis of measured *CPT* f_s and Δu_2 per the method of Takesue, et al. (1998) and the end bearing capacity based upon the approach of Eslami & Fellenius (1997) using the effective tip stress (q_t-u_2). The soil-pile stiffness is obtained from the shear wave measurement and the modulus reduction procedure per (33) utilized in an elastic continuum analysis of the axially-loaded pile. The comparison of measured and predicted axial pile response is shown in Figure 39. In addition to giving nonlinear load-displacement-capacity representation, the associated load-transfer for the drilled shaft is also obtained with good agreement.

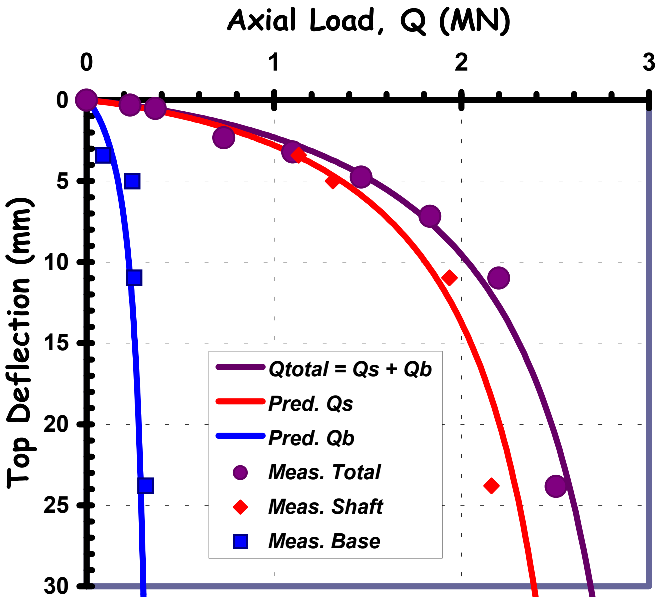

Figure 39. Measured & predicted Q-δ from SCPTu data.

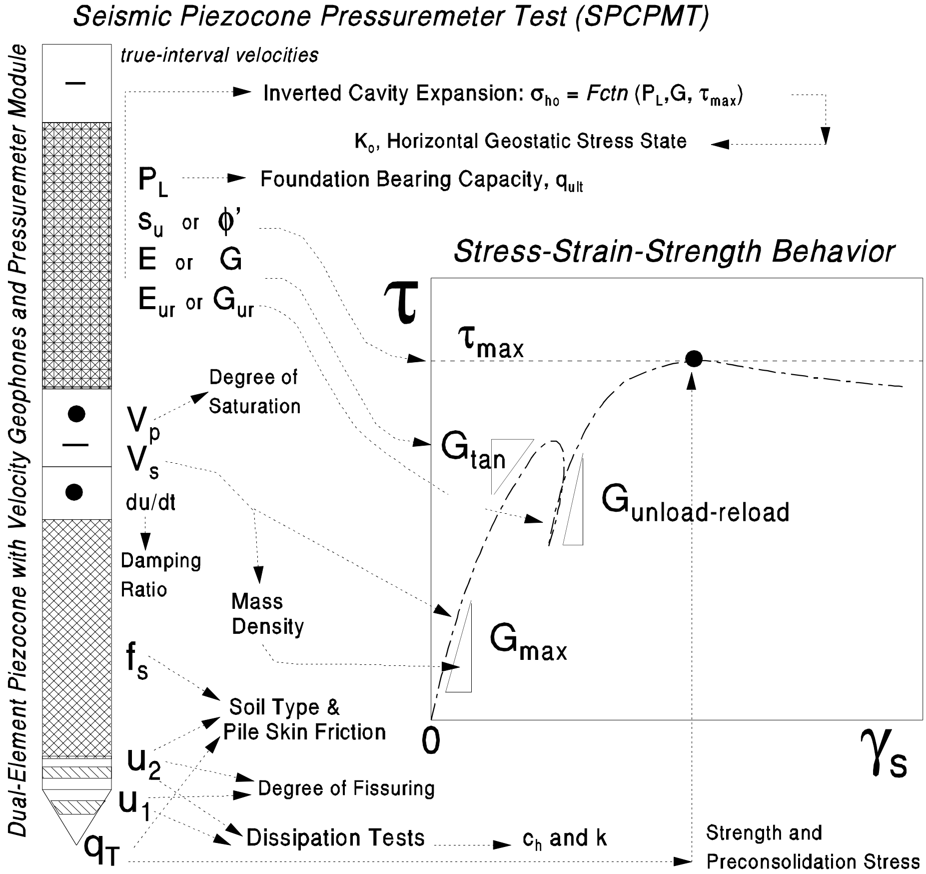

Figure 40. Concept of seismic piezocone pressuremeter with dissipation phases for site exploration.

8 CONCLUSIONS

Results from hybrid penetration tests (SCPTu and SDMT) incorporating downhole geophysics and dissipation phases provide an optimization for data collection during field exploration since information is collected at two opposite ends of the stress-strain-strength curve. The data can be utilized to evaluate the geostratigraphy and soil parameters including: unit weight (γ_t), effective strength parameters (ϕ'), total stress parameters (s_u), stress history (OCR and σ_p'), geostatic horizontal stresses (K_0), small-strain stiffness (G_{max}), intermediate-strain moduli (D′, E′, G′), and rigidity index (I_R), as well as the horizontal coefficient of consolidation (c_h) and permeability (k).

Direct measurements of stiffness at intermediate strains (i.e., cone pressuremeter) would be valuable in tailoring the fitting parameter of the modified hyperbola used here, or for more robust degradation and reduction schemes (e.g., Puzrin & Burland, 1996, 1998). New directions for enhanced geotechnical site characterization might include the seismic piezocone pressuremeter (SCPMTu), as seen in Fig. 40, as well as added sensors such as dielectric (permittivity) and resistivity to further improve and optimize the amounts and types of data recorded.

9 ACKNOWLEDGMENTS

The author acknowledges the funding support received from the National Science Foundation (NSF), United States Geological Survey (USGS), the Mid-America Earthquake Center (MAE), International Association of Foundation Drilling (ADSC), and Federal Highway Administration (FHWA) towards research efforts on in-situ testing. Additional thanks to Alan Lutenegger and Dan Brown for providing access & data at the NGES sites at Amherst/MA and Opelika/AL.

10 REFERENCES

Burghignoli, A., Pane, V., and Cavalera, L. (1991). Modeling stress-strain-time behavior of natural soils: monotonic loading. *Proceedings*, 10th ECSMFE, Vol. 3, Firenze, (Balkema, Rotterdam), 959-979.

Burland, J.B. (1989). Small is beautiful: The stiffness of soils at small strains. *Canadian Geotechnical Journal*, Vol. 26 (4), 499-516.

Burns, S.E. and Mayne, P.W. (1996). Small- and high-strain soil properties using the seismic piezocone. *Transportation Research Record* 1548, Washington, D.C., 81-88.

Burns, S.E. and Mayne, P.W. (1998). Monotonic & dilatory pore-pressure decay during piezocone tests. *Canadian Geotechnical J.* 35 (6), 1063-1073.

Butcher, A.P. and Powell, J.J.M. (1995). The effects of geological history on the dynamic stiffness in soils. *Proceedings*, XI European Conf. SMFE, Vol. 1, Copenhagen, 1.27-1.36.

Campanella, R.G. and Robertson, P.K. (1991). Use and interpretation of a research dilatometer. *Canadian Geotechnical J.* 28 (1), 113-126.

Campanella, R.G. (1994). Field methods for dynamic geotechnical testing. *Dynamic Geotechnical Testing II* (STP 1213), ASTM, West Conshohocken, PA., 3-23.

Campanella, R.G. and Robertson, P.K. (1988), "Current status of the piezocone test", *Penetration Testing 1988*, Vol. 1 (Proc. ISOPT-1, Orlando), Balkema, Rotterdam, 93-116.

Chen, B.S-Y. and Mayne, P.W. (1996). Statistical relationships between piezocone measurements and stress history of clays. *Canadian Geotechnical J.* 33 (3), 488-498.

Dahlberg, R. (1974). Penetration, pressuremeter, and screw plate tests in a preloaded natural sand deposit. *Proceedings*, ESOPT, Vol. 2.2, Stockholm, 68-87.

Diaz-Rodriguez, J.A., Leroueil, S., and Aleman, J. (1992). Yielding of Mexico City clay and other natural clays. *Journal of Geotechnical Engineering* 118 (7), 981-995.

DeGroot, D.J. and Lutenegger, A.J. (1994). A comparison between field and lab measurements of hydraulic conductivity in a varved clay. *Hydraulic Conductivity & Waste Contaminant Transport in Soil* (STP 1142), ASTM, West Conshohocken/PA, 300-317.

Duncan, J.M. and Chang, C.Y. (1970). Nonlinear analysis of stress and strain in soils. *Journal of the Soil Mechanics and Foundations Division*, ASCE, 96 (SM5), 1629-1653.

Eslami, A. and Fellenius, B.H. (1997). Pile capacity by direct CPT methods. *Canadian Geotechnical J.* 34 (6), 886-904.

Fahey, M. and Carter, J.P. (1993). A finite element study of the pressuremeter test in sand using a nonlinear elastic plastic model. *Canadian Geotechnical Journal* 30 (2), 348-362.

Fahey, M., Robertson, P.K, and Soliman, A.A. (1994). Towards a rational method of predicting settlements of spread footings on sand. *Vertical & Horizontal Deformations of Foundations & Embankments* (GSP 40), Vol. 1, ASCE, Reston, 598-611.

Finke, K.A., Mayne, P.W., and Klopp, R.A. (2001). Piezocone penetration testing in Atlantic Piedmont residuum. *Journal of Geotechnical & Geoenvironmental Engrg*. 127 (1), 48-54.

Fioravante, V., Jamiolkowski, M., and LoPresti, D.C.F. (1998). Assessment of the coefficient of earth pressure at rest from shear wave velocity. Geotechnique 48 (5), 657-666.

Hardin, B.O. and Drnevich, V.P. (1972). Shear modulus and damping in soils. *Journal of the Soil Mechanics and Foundations Division*, ASCE, 98 (7), 667-692.

Hatanaka, M. and Uchida, A. (1996). Empirical correlation between penetration resistance and ϕ of sandy soils. *Soils & Foundations* 36 (4), 1-9.

Hepton, P. (1988). Shear wave velocity measruemetns during penetration testing. *Penetration Testing in the U.K.*, Thomas Telford, London, 275-278.

Huang, A.B. (1991). Piezoblade tests in a clay calibration chamber. *Calibration Chamber Testing*, Elsevier, New York, 161-173.

Jamiolkowski, M., Ladd, C.C., Germaine, J. and Lancellotta, R. (1985), "New developments in field and lab testing of soils", *Proceedings*, 11th Intl. Conference on Soil Mechanics and Foundations Engineering, Vol. 1, San Francisco, 57-154.

Jamiolkowski, M., Lancellotta, R., LoPresti, D.C.F., and Pallara, O. (1994). Stiffness of Toyoura sand at small and intermediate strain. *Proceedings*, 13th Intl. Conf. on Soil Mechanics and Foundation Engrg (1), New Delhi, 169-172.

Jardine, R.J., Potts, D.M., St.John, H.D., and Hight, D.W. (1991). Some practical applications of a nonlinear ground model. *Proceedings*, 10th European Conference on Soil Mechanics and Foundation Engineering (1), Firenze, 223-228.

Keaveny, J. and Mitchell, J.K. (1986). Strength of fine-grained soils using the piezocone. Use of In-Situ Tests in Geotechnical Engrg. (GSP 6), ASCE, Reston/VA, 668-685.

Kulhawy, F.H. and Mayne, P.W. (1990). Manual on estimating soil properties for foundation design. *Report EL-6800.* Electric Power Research Institute, Palo Alto, 306 p.

Ladd, C.C. (1991). Stability evaluation during staged construction. ASCE *Journal of Geotechnical Engineering* 117 (4), 540-615.

Larsson, R. and Mulabdić, M. (1991a). Shear moduli in Scandinavian clays. *Report No. 40,* Swedish Geotechnical Institute, Linköping, 127 p.

Larsson, R. and Mulabdić, M. (1991b). Piezocone tests in clay. *Report No. 42*, Swedish Geotechnical Institute, Linköping, 240 p.

LoPresti, D.C.F., Pallara, O., Lancellotta, R., Armandi, M., and Maniscalco, R. (1993). Monotonic and cyclic loading behavior of two sands at small strains. ASTM *Geotechnical Testing Journal* 16 (4), 409-424.

LoPresti, D.C.F., Pallara, O., and Puci, I. (1995). A modified commercial triaxial testing system for small-strain measurements. ASTM *Geotechnical Testing Journal*, Vol. 18 (1), 15-31.

Lunne, T., Powell, J.J.M., Hauge, E.A., Mokkelbost, K.H., and Uglow, I.M. (1990). Correlation for dilatometer readings with lateral stress in clays. *Transportation Research Record* 1278, Wash, D.C., 183-193.

Lunne, T., Lacasse, S., and Rad, N.S. (1994). General report: SPT, CPT, PMT, and recent developments in in-situ testing. *Proceedings,* 12th ICSMFE, Vol. 4, Rio de Janeiro, 2339-2403.

Lunne, T., Robertson, P.K., and Powell, J.J.M. (1997). *Cone Penetration Testing in Geotechnical Practice*. Blackie Academic/Chapman-Hall Publishers, U.K.; available from EF Spon/Routledge Pub., New York, 312 p.

Lutenegger, A.J. (2000). NGES at Amherst, Massachusetts. *National Geotechnical Experimentation Sites* (GSP 93), ASCE, Reston, Virginia.

Marchetti, S. (1980). In-situ tests by flat dilatometer. *Journal of Geotechnical Engineering* 107 (GT3), 832-837.

Marchetti, S. (1985). On the field determination of Ko in sand. *Proceedings,* 11th ICSMFE, Vol. 5, San Francisco, 2667-2672.

Marchetti, S. (1997). The flat dilatometer: design applications. *Proceedings*, 3rd Geotechnical Engineering Conference, Cairo University, 1-25.

Martin, G.K. and Mayne, P.W. (1997). Seismic flat dilatometer tests in Connecticut Valley varved clay. ASTM *Geotechnical Testing Journal*, Vol. 20 (3), 357-361.

Mayne, P.W. and Kulhawy, F.H. (1982). Ko-OCR relationships in soil. *Journal of Geotechnical Engineering* 108 (GT6), 851-872.

Mayne, P.W. and Mitchell, J.K. (1988). Profiling of OCR in clays by field vane. *Canadian Geotechnical Journal* 25 (1), 150-157.

Mayne, P.W. and Bachus, R.C. (1989). Penetration pore pressure in clay by CPTu, DMT, and SBP. *Proceedings*, 12th ICSMFE, Vol. 1, Rio de Janeiro, 291-294.

Mayne, P.W., Kulhawy, F.H., and Kay, J.N. (1990), Observations on the development of pore water stresses during piezocone tests in clays. *Canadian Geotechnical J.* 27 (4), 418-428.

Mayne, P.W. and Kulhawy, F.H. (1990). Direct & indirect determinations of in-situ Ko in clays. *Transportation Research Record* 1278, National Acad. Press, 141-149.

Mayne, P.W. (1991). Determination of OCR in clays by piezocone tests using cavity expansion and critical state concepts. *Soils and Foundations*, Vol. 31 (2), 65-76.

Mayne, P.W. (1993). In-situ determination of clay stress history by piezocone model. *Predictive Soil Mechanics*, Thomas Telford, London, 483-495.

Mayne, P.W. and Chen, B.S-Y. (1994). Preliminary calibration of PCPT-OCR model for clays. *Proceedings*, 13^{th} International Conf. on Soil Mechanics and Foundation Engineering, Vol. 1, New Delhi, India, 283-286.

Mayne, P.W., Mitchell, J.K., Auxt, J., and Yilmaz, R. (1995). U.S. national report on the CPT. *Proceedings, CPT'95*, Vol. 1, Swedish Geotechnical Society, Linköping, 263-276.

Mayne, P.W. (1995). Profiling yield stresses in clays by in-situ tests. *Transportation Research Record* 1479, National Academy Press, Washington, D.C., 43-50.

Mayne, P.W. (1995). CPT determination of OCR and Ko in clean quartz sands. *Proceedings, CPT'95*, Vol. 2, Swedish Geotech Society, Linkoping, 215-220.

Mayne, P.W. and Dumas, C. (1997). Enhanced in-situ geotechnical testing for bridge foundation analysis. *Transportation Research Record* 1569, Wash, D.C., 26-35.

Mayne, P.W. (1998). Site characterization aspects of Piedmont residual soils in eastern United States. *Proceedings*, 14th International Conference on Soil Mechanics & Foundation Engineering, Vol. 4, Hamburg; Balkema, Rotterdam, 2191-2195.

Mayne, P.W., Robertson, P.K., and Lunne, T. (1998). Clay stress history evaluated from seismic piezocone tests. *Geotechnical Site Characterization*, Vol. 2, Balkema, Rotterdam, 1113-1118.

Mayne, P.W. and Martin, G.K. (1998). Commentary on Marchetti flat dilatometer correlations in soils. ASTM *Geotechnical Testing Journal*, Vol. 21 (3), 222-239.

Mayne, P.W., Schneider, J.A., and Martin, G.K. (1999). Small- and large-strain soil properties from seismic flat plate dilatometer tests. *Pre-Failure Deformation Characteristics of Geomaterials*, Vol. 1, (Torino), Balkema, Rotterdam, 419-426.

Mesri, G. and Abdel-Ghaffar, M.E.M. (1993). Cohesion intercept in effective stress stability analysis. *Journal of Geotechnical Engineering* 119 (8), 1229-1249.

Ohta, H., Nishihara, A., and Morita, Y. (1985). Undrained stability of Ko-consolidated clays. *Proceedings*, 11^{th} ICSMFE, Vol. 2, San Francisco, 613-616.

Olsen, R. and Mitchell, J.K. (1995). CPT stress normalization and prediction of soil classification. *Proceedings, Symposium CPT'95*, Vol. 2, Swedish Geotechnical Society, Linkoping, 257-262.

Pane, V., Manassero, M., Brignoli, E., and Soccodato, C. (1995). Cone penetration testing in Italy. *Proceedings, CPT'95*, Vol. 1, Linkoping, 101-114.

Parez, L. and Faureil, R. (1988). Le piézocône. Améliorations apportées à la reconnaissance de sols. *Revue Française de Géotech*, Vol. 44, 13-27.

Pool, R.G. (1994). Rational framework for interpreting OCR, undrained strength, and Ko from flat dilatometer tests in clay. *MS Thesis*, School of Civil & Environmental Engineering, Georgia Institute of Technology, Atlanta, 262 p.

Prevost, J.H. and Keane, C.M. (1990). Shear stress-strain curve generation from simple material parameters. *Journal of Geotechnical Engineering* 116 (8), 1255-1263.

Puzrin, A.M. and Burland, J.B. (1996). A logarithmic stress-strain function for rocks and soils. *Geotechnique* 46 (1), 157-164.

Puzrin, A.M. and Burland, J.B. (1998). Nonlinear model of small-strain behavior of soils. *Geotechnique* 48 (2), 217-233.

Robertson, P.K. and Campanella, R.G. (1983). Interpretation of cone penetration tests: sands. *Canadian Geotechnical Journal*, Vol. 20 (4), 719-733.

Robertson, P.K., Campanella, R.G., Gillespie, D., and Rice, A. (1986). Seismic CPT to measure in-situ shear wave velocity. *Journal of Geotechnical Engineering* 112 (8), 71-803.

Robertson, P.K., Campanella, R.G., Davies, M.P., and Sy. A. (1988). Axial capacity of driven piles in deltaic soils using CPT. *Penetration Testing 1988*, Vol. 2, Balkema, Rotterdam, 919-928.

Robertson, P.K. (1990). Soil classification using the cone penetration test. *Canadian Geotechnical J.* 27 (1), 151-158.

Schmertmann, J.H. (1986). Suggested method for performing the flat dilatometer test. ASTM *Geotechnical Testing J.* 9 (2), 93-101.

Schneider, J.A., Hoyos, L., Mayne, P.W., Macari, E.J., and Rix, G.J. (1999). Field & lab measurements of dynamic shear modulus of Piedmont residuum. *Behavioral Characteristics of Residual Soils* (GSP 92), ASCE, Reston/Virginia, 12-25.

Senneset, K., Sandven, R. and Janbu, N. (1989). Evaluation of soil parameters from piezocone tests. *Transportation Research Record* 1235, Natl. Acad. Press, 24-37.

Shibuya, S., Tatsuoka, F., Teachavorasinskun, S., Kong, X., Abe, F. (1992). Elastic deformation properties of geomaterials. *Soils and Foundations* 32 (3), 26-46.

Smith, P.R., Jardine, R.J., and Hight, D.W. (1992). The yielding of Bothkennar clay. *Geotechnique* 42 (2), 257-274.

Sully, J.P. and Campanella, R.G. (1995). Evaluation of in-situ anisotropy from crosshole & downhole. *Geotechnique* 45 (2), 267-282.

Takesue, K., Sasao, H., and Matsumoto, T. (1998). Correlation between ultimate pile skin friction and CPT data. *Geotechnical Site Characterization*, Vol. 2, Balkema, Rotterdam, 1177-1182.

Tatsuoka, F. and Shibuya, S. (1992). Deformation characteristics of soils and rocks from field and laboratory tests. *Rept. of the Institute of Industrial Science*, Vol. 37, No. 1, Univ. of Tokyo, 136 p.

Tatsuoka, F., Jardine, R.J., LoPresti, D.C.F., DiBenedetto, H., and Kodaka, T. (1997). Theme Lecture: Characterizing the pre-failure deformation properties of geomaterials. *Proceeedings*, 14th Intl. Conf. on Soil Mechanics & Foundation Engineering, Vol. 4, Hamburg, 35 p

Teachavorasinskun, S., Shibuya, S. and Tatsuoka, F. (1991). Stiffness of sands in monotonic & cyclic torsional simple shear. *Geotechnical Engineering Congress*, Vol. II (Boulder), GSP No. 27, ASCE, New York, 863-878.

Teh, C.I. and Houlsby, G.T. (1991). An analytical study of the cone penetration test in clay. Geotechnique 41 (1), 17-34.

Vucetic, M. and Dobry, R. (1991). Effect of soil plasticity on cyclic response. *Journal of Geotechnical Engineering* 117 (1), 89-107.

Wroth, C.P. (1984). The interpretation of in-situ soil tests. (The 24th Rankine Lecture). *Geotechnique*, Vol. 34 (4), 449-489.

Wroth, C.P. and Houlsby, G.T. (1985). Soil mechanics: property characterization & analysis procedures. *Proceedings*, 11^{th} ICSMFE, Vol. 1, San Francisco, 1-56.